Phytochemistry 156 (2018) 55–72

Contents lists available at ScienceDirect

Phytochemistry

journal homepage: www.elsevier.com/locate/phytochem

Unusual subunits are directly involved in binding substrates for natural rubber biosynthesis in multiple plant species

Katrina Cornish[a,c,*,1], Deborah J. Scott[a,1], Wenshuang Xie[a], Christopher J.D. Mau[a], Yi Feng Zheng[b], Xiao-hui Liu[b], Glenn D. Prestwich[b]

[a] USDA-ARS Western Regional Research Center, 800 Buchanan Street, Albany, CA 94710, USA
[b] Department of Medicinal Chemistry, The University of Utah, South 2000 East, Rm. 307, Salt Lake City, UT 84112, USA
[c] Center of Applied Plant Sciences, Institute of Materials Research, Institute of Humanitarian Engineering, Department of Chemistry and Biochemistry, USA

ARTICLE INFO

Keywords:
Allylic pyrophosphate
Benzophenone
Enzyme complex
Natural rubber
Rubber transferase

ABSTRACT

Rubber particles from rubber-producing plant species have many different species-specific proteins bound to their external monolayer biomembranes. To date, identification of those proteins directly involved in enzymatic catalysis of rubber polymerization has not been fully accomplished using solubilization, purification or reconstitution approaches. In an alternative approach, we use several tritiated photoaffinity-labeled benzophenone analogs of the allylic pyrophosphate substrates, required by rubber transferase (RT-ase) to initiate the synthesis of new rubber molecules, to identify the proteins involved in catalysis.

Enzymatically-active rubber particles were purified from three phylogenetically-distant rubber producing species, *Parthenium argentatum* Gray, *Hevea brasiliensis* Muell. Arg, and *Ficus elastica* Roxb., each representing a different Superorder of the Dicotyledonae. Geranyl pyrophosphate with the benzophenone in the *para* position (Bz-GPP(*p*)) was the most active initiator of rubber biosynthesis in all three species. When rubber particles were exposed to ultra-violet radiation, 95% of RT-ase activity was eliminated in the presence of 50 μM Bz-GPP(*p*), compared to only 50% of activity in the absence of this analog. ^{3}H-Bz-GPP(*p*) then was used to label and identify the proteins involved in substrate binding and these proteins were characterized electrophoretically.

In all three species, three distinct proteins were labeled, one very large protein and two very small proteins, as follows: *P. argentatum* 287,000, 3,990, and 1,790 Da; *H. brasiliensis* 241,000, 3,650 and 1,600 Da; *F. elastica* 360,000, 3,900 and 1,800 Da. The isoelectric points of the *P. argentatum* proteins were 7.6 for the 287,000 Da, 10.4 for the 3,990 Da and 3.5 for the 1,790 Da proteins, and of the *F. elastica* proteins were 7.7 for the 360,000 Da, 6,0 for the 3,900 Da, and 11.0 for the 1,800 Da proteins. *H. brasiliensis* protein pI values were not determined.

Additional analysis indicated that the three proteins are components of a membrane-bound complex and that the ratio of each small protein to the large one is 3:1, and the large protein exists as a dimer. Also, the large proteins are membrane bound whereas both small proteins are strongly associated with the large proteins, rather than to the rubber particle proteolipid membrane.

1. Introduction

Rubber transferase (EC 2.5.1.20) is a membrane-bound *cis*-prenyl transferase, which produces polymers of indeterminate length between 50,000 and greater than 1,000,000 g/mol. It is well established that rubber transferase (RT-ase) is bound to cytoplasmic rubber particles (RPs), with an unconventional proteolipid monolayer membrane (Siler et al., 1997; Cornish et al., 1999; Wood and Cornish, 2000). The ability to make rubber is widespread across eudicotyledonous plants and rubber particles have species-specific complements of lipids and proteins complicating the identification of RT-ase (Siler et al., 1997). *H. brasiliensis* rubber particles are especially complex with hundreds of different associated proteins.

Several different proteins have been implicated as playing a role in rubber molecule formation, including a high molecular weight, hydrophobic, integral membrane, dimeric glycoprotein (LPR) in *F. elastica* rubber particles (Siler and Cornish, 1993; Cornish et al., 1994). Large rubber particle bound proteins also were found and characterized in *P.*

* Corresponding author. Current address: The Ohio State University, 1680 Madison Avenue, Wooster, OH 44691, USA.
E-mail address: cornish.19@osu.edu (K. Cornish).
[1] Cornish and Scott are co-first authors

https://doi.org/10.1016/j.phytochem.2018.08.014
Received 10 May 2018; Received in revised form 31 July 2018; Accepted 17 August 2018

argentatum and *H. brasiliensis* (Cornish et al., 1993; Siler and Cornish, 1994). Other rubber particle-bound proteins which may be involved include the small rubber particle protein (SRPP) and related rubber elongation factor (REF) (Dennis and Light, 1989; Schmidt et al., 2010b; Berthelot et al., 2014; Laibach et al., 2015; Tong et al., 2017; Wadeesirisak et al., 2017). Various soluble *cis*-prenyl transferases also have been proposed (Post et al., 2012; Qu et al., 2015; Light and Dennis, 1989; Light et al., 1989) although definitive proof of a role as RT-ase is lacking. Most recently, RT-ase activity was reconstituted in *H. brasiliensis* RP's which had been inactivated using detergents to partially deproteinize the RPs (Yamashita et al., 2016). However, activity could not be reconstituted in liposomes, suggesting that either structural or other essential proteins remaining on the detergent-treated RPs are essential to RT-ase activity.

Purification of enzymatic activity away from the rubber particle membrane has been difficult because of loss of structural integrity and the need for an aqueous-organic interface to maintain the reaction. Solubilization attempts often entrap proteins as particles collapse and coagulate. Two proteins solubilized from the *P. argentatum* RP membrane (52,000 and 130,000 Da) may be involved in rubber biosynthesis in *P. argentatum* (Benedict et al., 1990; Madhavan et al., 1989) but the solubilized activity reported has not been repeated. Early reports of solubilized activity in *H. brasiliensis* appear to have been the result of inadvertently adding an initiator system rather than RT-ase enzyme to the assay system (see reviews in (Cornish, 1993; Cornish and Siler, 1996)).

Due to the difficulty of purifying enzymatically-active RT-ase, a functional labeling approach was used, in this report, as a prelude to protein identification. Benzophenone photophore biochemical probes (Dorman and Prestwich, 2000), have been extensively used in chemistry and biology over the past two decades and comprehensively reviewed (Dorman et al., 2016). Benzophenone derivatives of allylic pyrophosphates (Dorman and Prestwich, 1994), were successfully used in two distinct isoprenoid enzyme groups, the bacterial prenyltransferases (Marecak et al., 1997; Zhang et al., 1998) and the protein prenyltransferases from yeast (Gaon et al., 1996a,b; Turek-Etienne et al., 2003) and mammals (Ying et al., 1994). The allylic pyrophosphate initiator binding site of the RT-ases of both *H. brasiliensis* and *P. argentatum* share similar chemical preferences to the FPP binding site of protein farnesyltransferases, and inhibitors of the protein farnesyltransferase also inhibit the RT-ases of *P. argentatum* and *H. brasiliensis* (Mau et al., 2003). This similarity means benzophenone APPs, which act as substrates in protein farnesyltransferase, will likely also act as substrates for RT-ase.

In this paper, we describe the use of APPs covalently attached to benzophenones by ether linkage (Marecak et al., 1997) as photo affinity labeled substrates of RT-ase, and, when tritiated, as biochemical probes to identify proteins directly involved in the catalytic reaction of rubber biosynthesis. These experiments are performed using enzymatically-active rubber particles purified from three phylogenetically divergent species, because we reason that their kinetically similar RT-ases (Cornish, 2001a,b) will also be structurally similar. We report on the characterization of the labeled proteins and propose a preliminary architecture of the RT-ase enzyme complex, which appears to be largely conserved across the Eudicot clade of the plant kingdom.

2. Results

2.1. Benzophenones as allylic pyrophosphate initiators of rubber polymerization

When the benzophenone (Bz) allylic pyrophosphate (APP) substrate analogs (Fig. 1) were tested for their effectiveness as initiators of rubber biosynthesis, RT-ases from all three species were able to incorporate IPP into new rubber (Fig. 2). The IPP incorporation rates initiated by Bz-GPP(*p*) and Bz-FPP(*m*) were at least as high as the IPP incorporation rate initiated by *E,E*-FPP, the natural initiator *in vivo*. Within each species, the V_{max}'s for Bz-GPP(*p*), Bz-FPP(*m*) and *E,E*-FPP were similar (Table 1), except that the $V_{max}^{\text{Bz-GPP}(p)}$ for *H. brasiliensis* was 155% of the $V_{max}^{E,E\text{-FPP}}$. The *H. brasiliensis* RT-ase was able to use Bz-DMAPP (*m*) and (*p*) to initiate IPP incorporation at a very similar rate to *E,E*-FPP, as well. However, for *F. elastica* and *P. argentatum*, the RT-ase velocities in Bz-DMAPP(*m*) and Bz-DMAPP(*p*) were substantially lower than those with *E,E*-FPP (Table 1).

When the K_m's (Table 1) of the Bz-APP initiators were compared to *E,E*-FPP, species-dependent variations became clear. In *F. elastica*, the maximum variation in K_m was only a factor of three, while in *H. brasiliensis* and *P. argentatum*, the variation in K_m was much greater, factors of 50 and 15, respectively. The K_m's of all the Bz-APP initiators in *H. brasiliensis* were considerably lower than the K_m for *E,E*-FPP. In fact, the K_m's for both Bz-DMAPP(*p*) and Bz-GPP(*p*) were as low as those found for *E,E*-FPP in *P. argentatum*, indicating a very high affinity of the RT-ase for these substrates. In addition, the relative binding affinities of the RT-ases for the different APP initiators were different among the three species. The affinity orders were as follows:

F. elastica

$$K_m^{\text{Bz-DMAPP}(m)} = K_m^{\text{Bz-DMAPP}(p)} < K_m^{\text{Bz-GPP}(p)} = K_m^{E,E\text{-FPP}} < K_m^{\text{Bz-FPP}(m)}.$$

H. brasiliensis

$$K_m^{\text{Bz-DMAPP}(p)} < K_m^{\text{Bz-GPP}(p)} < K_m^{\text{Bz-FPP}(m)} < K_m^{\text{Bz-DMAPP}(m)} < K_m^{E,E\text{-FPP}}.$$

P. argentatum

$$K_m^{E,E\text{-FPP}} < K_m^{\text{Bz-DMAPP}(m)} < K_m^{\text{Bz-DMAPP}(p)} = K_m^{\text{Bz-FPP}(m)} < K_m^{\text{Bz-GPP}(p)}.$$

2.2. Inhibition of activity by UV

2.2.1. Time

The UV light exposure necessary to inactivate RT-ase activity by photo affinity labeling was determined for the Bz-APP initiator, Bz-GPP (*p*) in all three species. Bz-DMAPP(*p*) also was tested but only in *H. brasiliensis*. The percentage of remaining RT-ase activity in washed (purified) (WRP) after UV light exposure time (Fig. 3) indicated that 70% of activity was lost from all three RT-ases after 5 min of UV light exposure in Bz-GPP(*p*) compared to the non-illuminated controls. During the same exposure time, RT-ase activity, assayed in the presence of *E,E*-FPP, was not inhibited, and 5 min of UV exposure seemed to slightly enhance activity of the *F. elastica* and *H. brasiliensis* RT-ases.

Maximum inhibition levels were reached in *P. argentatum* after 15 min (Fig. 3c), but 30 min were required to fully inhibit RT-ase activity in *F. elastica* (Fig. 3a) and *H. brasiliensis* (Fig. 3b). Bz-DMAPP(*p*) required approximately double the UV exposure time to inhibit the *H. brasiliensis* RT-ase to the same degree as Bz-GPP(*p*) (Fig. 3b).

It is also clear from the UV exposure of the *E,E*-FPP controls that prolonged exposure to UV light inhibited RT-ase activity. The *P. argentatum* RT-ase was the most sensitive to UV of the three enzymes, whereas the *H. brasiliensis* enzyme was the most resistant to UV light-induced inactivation. This is expected because the *P. argentatum* RT-ase is also the most temperature sensitive enzyme of the three (Cornish and Backhaus, 1990) due to its purification from tissue homogenates rather than tapped latex. Homogenization causes extensive release of degradative enzymes. UV light absorption, itself, damages proteins (and nucleic acids) and will eventually cause enzyme denaturation. Additional damage in the presence of the Bz-analogs is caused by reaction of the pi-pi star excited benzophenones' ketyl radicals non-specifically damaging proteins and lipids, and when the analogs covalently link to the proximal amino acids in the RT-ase active site they block access by other substrates (Dorman et al., 2016).

2.2.2. Concentration of Bz-GPP(p)

The three RT-ases selected to probe have similar but not identical

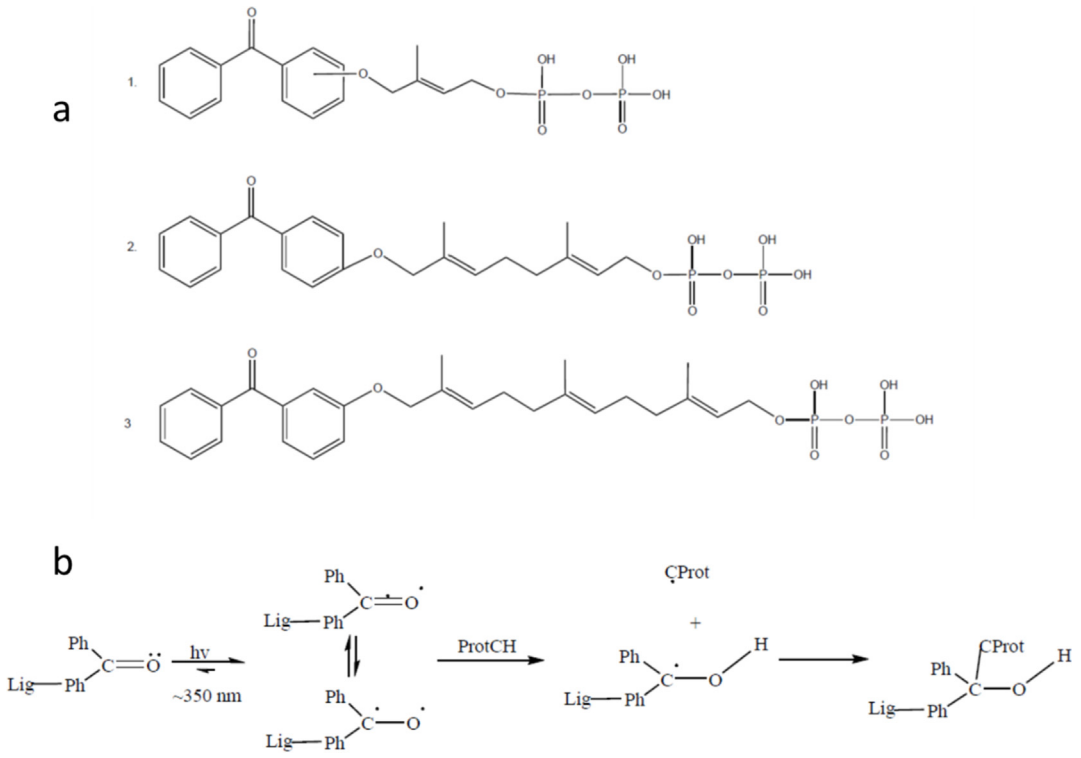

Fig. 1. a. Structures of the benzophenone allylic pyrophosphates: (1) Bz-DMAPP (*m*) or (*p*), (2) Bz-GPP (*p*), (3) Bz-FPP (*m*). b. Photochemistry of the benzophenone in photo affinity labeling (copied from Fig. 5a (34)).

reaction kinetics with IPP and different APPs (Cornish, 2001a,b) and so assay, labelling and inactivation conditions were optimized for each (see). In the absence of UV light, Bz-GPP(*p*) may be slightly less effective as an initiator than *E,E*-FPP in *F. elastica* and *P. argentatum* than in *H. brasiliensis* (Fig. 4). There also appeared to be concentration differences, with a larger discrepancy in RT-ase activity between the two initiators at 10 µM and 100 µM in *F. elastica* (Fig. 4a) and *P. argentatum* (Fig. 4c). In contrast, *H. brasiliensis* RT-ase activity was considerably higher when initiated by Bz-GPP(*p*) than by *E,E*-FPP at initiator concentrations of ≤10 µM. However, as the initiator concentration increased to 100 µM, the activity of the RT-ase in Bz-GPP(*p*) decreased to match the activity with *E,E*-FPP alone.

After exposure to UV light, the IPP incorporation rate by the *F. elastica* (Fig. 4a) and *P. argentatum* (Fig. 4c) RT-ases dropped below their FPP controls between 10 and 100 µM Bz-GPP(*p*). The *H. brasiliensis* RT-ase activity began to decline even at the lowest Bz-GPP(*p*) concentrations, dropping below the activity in FPP at 1 µM, and continued to decline out to 100 µM Bz-GPP(*p*) (Fig. 4b).

Based on these results, 50 µM Bz-GPP(*p*) was selected as the best substrate and concentration to use to further optimize the experimental conditions for labeling proteins on WRP from *F. elastica*, *H. brasiliensis* and *P. argentatum*.

2.2.3. Presence or absence of allylic-PP initiator, E,E-FPP, during UV exposure

In *H. brasiliensis* WRP, the presence or absence of *E,E*-FPP initiator during UV exposure had little impact on the RT-ase activity remaining after 60 min (Fig. 3b). However, 50% of RT-ase activity was lost in the absence of *E,E*-FPP (Fig. 4b), just slightly lower than that observed in *E,E*-FPP.

2.2.4. Determination of rubber particle concentrations for the photoaffinity labeling assay

RT-ase activity in a 50 µl reaction mixture containing 12 mg *H. brasiliensis* WRP (4.49 µmol IPP/mg WRP/4 h) was not inhibited by 60 min exposure UV light (4.38 µmol IPP/mg WRP/4 h) (data not shown). The density of the particles seemed to protect the RT-ase from UV damage. When 100 µM Bz-GPP was added, the activities with and without exposure to UV light, 4.172 and 1.847 µmol IPP/mg WRP/4 h, respectively, showed 65% inhibition after 60 min (data not shown). With the protection afforded by the increased density, the UV light exposure caused the same level of inhibition after 60 min with 12 mg WRP per 50 µl as 15 min with 1 mg WRP per 50 µl (data not shown).

2.2.5. Incorporation of ^{3}H-Bz-GPP(p)

The detection limit of the imaging scanner used in this study was 1000 dpm per band or minimally 10,000 dpm per reaction (one lane per reaction). Thus, each reaction required 0.2 to 0.02 nmoles of labeled substrate, because the specific activity of the substrate ranged between 0.05 dpm/fmol to 0.5 dpm/fmol. The total amount of tritium associated with proteins ranged from 1102 cpm/20 min/6 µl added ^{3}H BzGPP(*p*) to 65133 cpm/6 µl ^{3}HBzGPP(*p*). 12.2 cpm/min/6 µl reflects less than 0.02% incorporation of the substrate into rubber. Using *H. brasiliensis* WRP, three concentrations of ^{3}HBz-GPP (1 µM (0.05 nmol), 10 µM (0.5 nmol) and 50 µM (2.5 nmol)), and a 60 min UV light exposure, incorporated 10,000 dpm/mg WRP in the presence of 50 µM ^{3}HBz-GPP and caused a 33% inhibition of RT-ase activity (Table 2). Extrapolating for the number of benzophenones bound per rubber particle (one benzophenone per reaction with a protein molecule and Fig. 1b), it appeared that 2000 to 140,000 Bz molecules had bound per rubber particle (see Table 3).

2.3. Evaluation of radiolabeled proteins by gel electrophoresis and scanning

When enzymatically-active rubber particles purified from *H. brasiliensis* latex were exposed to UV light for 90 min in presence of ^{3}H-Bz-GPP, run on 4–20% acrylamide gels, and the scans compared with a silver stained duplicate gel, a highly specific labeling of proteins was observed (Fig. 5). Very similar labelling patterns were observed for *P. argentatum* and *F. elastica* (photographs not shown). The two separately

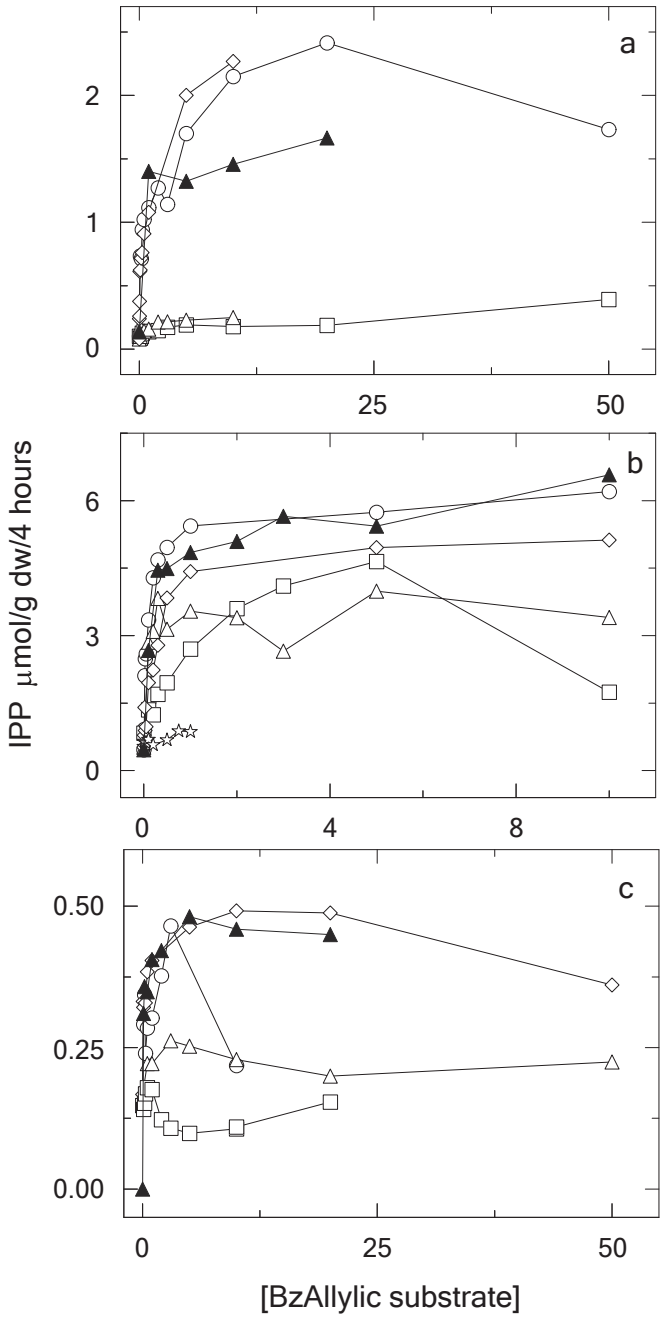

Fig. 2. Incorporation of ^{14}C-IPP by rubber transferase in purified rubber particles from (a) *F. elastica*, (b) *H. brasiliensis*, and (c) *P. argentatum* in the presence of different allylic pyrophosphate initiators (□) Bz-DMAPP (*m*), (Δ) Bz-DMAPP (*p*), (○) Bz-GPP (*p*), (◊) Bz-FPP (*m*), (φ) Bz-FPP (*p*) and (▲) *E,E*-FPP.

labeled peaks Rf's were: (a) *F. elastica* (17 and 60 mm), (b) *H. brasiliensis* (15 and 70 mm), and (c) *P. argentatum* (17 and 85 mm). The small protein band contained two distinct proteins which could be detected under strongly reducing conditions and could be readily separated by IEF (see below).

To determine if time of exposure to UV light affected which proteins were photo affinity labeled, and the amount of labeling which occurred, *P. argentatum* rubber particles were exposed for 5, 15, 30, 60 min, separated by gel electrophoresis on 4–20% gels and scanned (Fig. 6). The area under the peak at 110 mm doubled from between 5 and 30 min of UV exposure with little further increase between 30 and 60 min (Fig. 6). (The exact location on the gel depended upon the placement of the gel on the Bioscan plate.) The peak at 55 mm slightly decreased from 5 min to 15 min, and then slowly increased out to 60 min.

Table 1
Kinetic constants of benzophenone allylic pyrophosphates in *Ficus elastica*, *Hevea brasiliensis* and *Parthenium argentatum*.

Species	Benzophenone	V_{max} [a]	K_m (µM)
Ficus elastica	Bz-DMAPP (*m*)	0.2	0.1
	Bz-DMAPP (*p*)	0.2	0.1
	Bz-GPP (*p*)	1.5	0.2
	Bz-FPP (*m*)	1.9	0.3
	E,E-FPP	1.6	0.2
	All E-SPP	–	0.02
Hevea brasiliensis	Bz-DMAPP (*m*)	4.4	0.4
	Bz-DMAPP (*p*)	3.4	0.02
	Bz-GPP (*p*)	8.1	0.03
	Bz-FPP (*m*)	3.9	0.1
	E,E-FPP	5.2	0.96
	All E-SPP	5.0	0.65
Parthenium argentatum	Bz-DMAPP (*m*)	0.2	0.03
	Bz-DMAPP (*p*)	0.3	0.1
	Bz-GPP (*p*)	0.4	0.3
	Bz-FPP (*m*)	0.4	0.1
	E,E-FPP	0.5	0.02

[a] ^{14}C-IPP incorporation in µmoles/g dw/4 h, at 25 °C for *F. elastica* and *H. brasiliensis* and at 16 °C for *P. argentatum*.

2.3.1. Gel washing to determine persistence of label

The amount of ^{3}H labeling bound to the two small proteins was unaltered by extensive washing of the gels before drying. However, the ^{3}H labeling associated with the large proteins steadily declined with number of washes (data not shown).

2.3.2. Protein characterization

2.3.2.1. Molecular weight of large proteins. When the unlabeled large proteins of both *P. argentatum* and *H. brasiliensis* were run on 3.5 and 4.0% phosphate gels (Fig. 7), the proteins migrated quite a distance from the sizes predicted by standards. The tritiated large molecular weight proteins from each species were run on 3%, 3.5%, 4%, and 4.5% phosphate gels and scanned for 8 h (Fig. 8a), and Ferguson analysis (Fig. 8b and c) determined the molecular weight of these large proteins to be 360,000 Da for *F. elastica*, 241,000 Da for *H. brasiliensis* and 287,000 Da for *P. argentatum*.

The labeled portion of the *H. brasiliensis* and *P. argentatum* gels 4.0% and 4.5% were cut out, extracted and filtered. Samples were counted and run on a Novex 3–8% gel system. The proteins in the gel migrated in accordance with the molecular weights predicted by the Ferguson analysis (data not shown).

2.3.2.2. Molecular weight of small proteins. The molecular weight of the labeled small proteins from *H. brasiliensis* and *P. argentatum* was determined using 15%, 16.5%, 18% polyacrylamide gels and analyzed (Fig. 9). When the samples were run under reducing conditions, after heating in the presence of urea, two very small proteins were observed for all three species (Table 4). In less reducing environments, without urea, (samples analyzed in 15% gels) the size of the labeled proteins was substantially greater (14,000 Da), suggesting aggregation. These proteins can be seen for the three species together on a silver stained Novex gel 3–8% of WRP rubber particles (Fig. 10).

2.3.2.3. Isoelectric point of P. argentatum proteins. The isoelectric points (pI) of the *P. argentatum* labeled proteins were determined using 4% reverse IEF gels (Table 4). The smallest labeled protein of 1,500 Da, had a pI of 3.5. The protein dyed orange with silver stain. The other small molecular weight protein, which was 3,990 Da, was easily separated from the 1,500 protein by IEF because its pI was basic. The pI of this

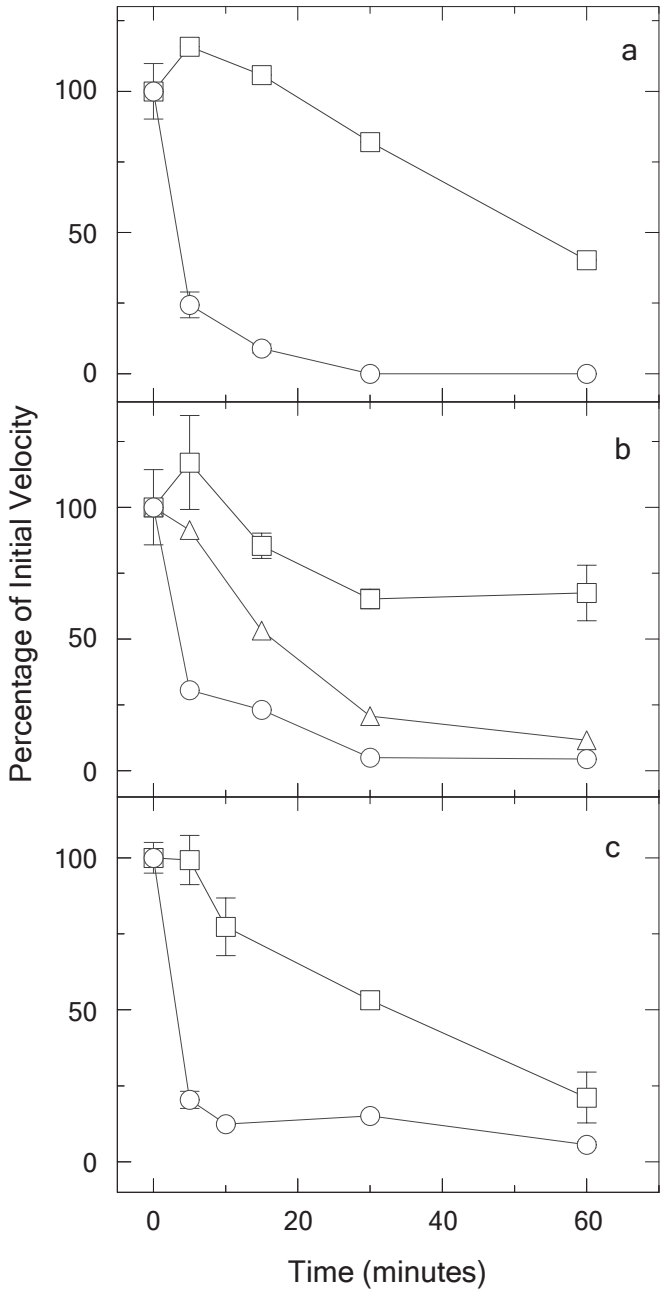

Fig. 3. Incorporation of ^{14}C-IPP by rubber transferases in purified rubber particles (WRP) of (a) *F. elastica* (1 mg WRP), (b) *H. brasiliensis* (1 mg WRP), and (c) *P. argentatum* (0.75 mg WRP) after 0, 5, 15, 30, and 60 min exposure to UV light in the presence of allylic pyrophosphate initiators (o, Bz-GPP (*p*); Δ, Bz-DMAPP (*p*); □, *E,E*-FPP. Reaction mixtures were irradiated with UV at 4 °C. After irradiation, IPP and *E,E*-FPP were added to assay the remaining rubber transferase activity and temperature was increased to 25 °C (16 °C, in the casse of *P. argentatum*). Substrate concentrations were: (a) *F. elastica* 50 μM Bz-GPP (*p*), 20 μM E,*E*-FPP and 5 mM IPP; (b) *H. brasiliensis* 10 μM Bz-GPP (*p*) or 4 μM Bz-DMAPP (*p*), 20 μM E,*E*-FPP and 5 mM IPP; *P. argentatum* 10 μM Bz-GPP, 20 μM E,*E*-FPP and 80 μM IPP (*p*).

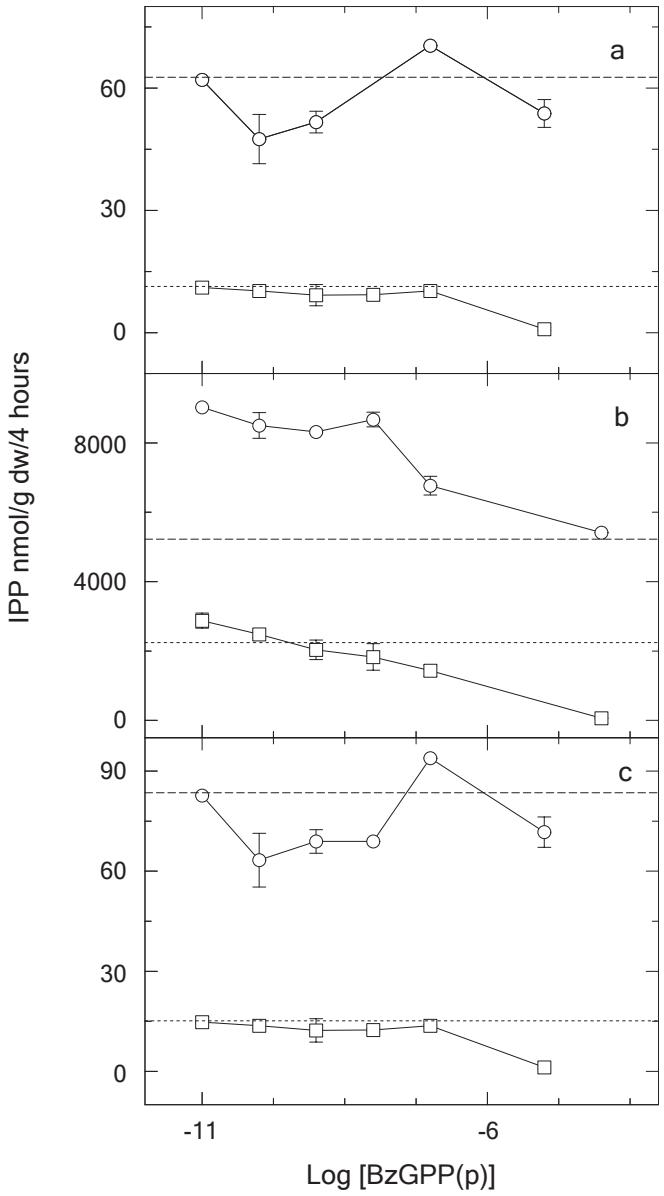

Fig. 4. Incorporation of ^{14}C-IPP by rubber transferases in purified rubber particles of (a) *F. elastica,* (b) *H. brasiliensis,* and (c) *P. argentatum* at concentrations from 10 pM to 100 μM Bz-GPP(*p*) before (o) and after (□) exposure to UV light for 60 min. Dashed lines indicate the ^{14}C-IPP incorporation rates in 20 μM E,*E*-FPP, before (—) and after exposure to UV (····). Rubber transferase activity was assayed at 25 °C for *F. elastica* and *H. brasiliensis* and at 16 °C for *P. argentatum* in 20 μM E,*E*-FPP and 5 mM IPP for *F. elastica*, 20 μM E,*E*-FPP and 1.5 mM IPP for *H. brasiliensis* and 20 μM E,*E*-FPP and 80 μM IPP for *P. argentatum*.

protein was determined from its amino acid sequence (four fragments of the complete protein) to be 10.5 (Table 4).

When an unlabeled sample of the large *P. argentatum* protein migrating at 280,000 Da (Fig. 11 a) was electroeluted and run on an IEF gel (Fig. 11 b), a strong association with two other proteins was observed. The strongest silver stain was associated with a protein with a pI of 6.3, which appears to be the 52 kD RPP. It has previously been shown that the large native protein had a large component of RPP subunits when run under denaturing conditions (Siler and Cornish, 1994). However, the 1,790 Da protein (pI 3.5) also was strongly stained. The 3,990 Da protein is not clearly separated on the IEF gel because its pI of 10.5 would have trapped it in the stacking gel (loading well), where a silver stained band is indeed visible (Fig. 11b). A third, more lightly stained protein had a pI of 7.5 and Rotafor separation electrophoretic analysis demonstrated that this protein was the intact large molecular weight protein.

2.3.3. Relative abundance of subunits in the rubber transferase complex

The relative abundance of the different subunits (compared to each other), and the percentage of label incorporated by the different subunits was calculated for *H. brasiliensis* and *P. argentatum* (Table 5) and used to determine the ratio of small subunits to large subunits (Table 6).

Table 2
Quantification of ^{3}H-Bz-GPP(*p*) incorporation by purified *Hevea brasiliensis* rubber particles in the presence and absence of EDTA, which chelates the Mg^{2+} activator and prevents IPP polymerization.

[3H Bz-GPP (*p*)]	Bz-GPP(*p*)	[EDTA]	Washes	Counts on filter		Bz-GPP(*p*) incorporation
(*μM*)	(*nmoles*)	(*mM*)	(*number*)	(*cpm/mg*)	*s.e.*	(*molecules/rubber particle*[a])
50	2.50	0	23	11,198	909	1.4×10^5
50	2.50	20	23	11,300	284	
10	0.50	0	14	1915	57	1.8×10^4
10	0.50	20	14	1755	201	
1	0.05	0	10	188	10	2.1×10^3
1	0.05	20	10	206	12	

[a] The concentration of rubber particles/mg is approximately 10^9. Tritium added as ^{3}H-Bz-GPP(*p*)was: 2.5 nmol, 164,881 cpm; 0.5 nmol, 40,577 cpm; 0.05 nmol, 3707 cpm. The counts per minutes (cpm)/mg are the means ± the standard error of the mean (s.e.).

Table 3
Rubber transferase activity of *Hevea brasiliensis* purified rubber particles.

[Bz-GPP(*p*)]	[FPP]	UV exposure	RT-ase activity
(*μM*)	(*μM*)	(*min*)	(*nmol IPP/g/4* h)
0	20	0	5874
50	20	0	3674
0	20	60	977
50	20	60	650

a. The concentration of rubber particles/mg is approximately 10^9. (For 2.5 nmol 164,881 cpm, for 0.5 nmol 40,577 cpm and for 0.05 nmol 3707 cpm.)

The maximum activation (n_{app}) of the RT-ases by two different APP substrates, and the concentration at which maximum activity occurs was determined (Table 7). The maximum substrate activation levels for *H. brasiliensis* and *P. argentatum* RT-ases, 3.6 and 2.6, respectively, were remarkably similar to the ratios of subunits determined by labeling quantification (Table 6).

3. Discussion

We found that several benzophenone substrates could initiate rubber biosynthesis with K_ms and V_{max}s similar to *E,E*-FPP, placing the three RT-ase enzymes investigated into the isoprenoid pyrophosphate synthase group, distinct from the protein prenyl transferases. As indicated previously from competition studies (Mau et al., 2003), the three RT-ases clearly had species-specific structural differences. The *H. brasiliensis* RT-ase rubber transferase preferred the *para* isomers to the *meta* isomers, and the benzophenone substituted APPs over *E,E*-FPP. In contrast, the *F. elastica* RT-ase preferred *E,E*-FPP over the Bz-FPP form, but otherwise had no isomer preference and preferred the smaller substituted APPs *i.e.* DMAPP more than GPP. *P. argentatum* RT-ase, on the other hand, preferred *E,E*-FPP above all the benzophenone derivatives. However, within the benzophenone derivatives, the *P. argentatum* RT-ase preferred the *meta* substitution to the *para*, and preferred DMAPP *meta* or *para* to benzophenone-substituted GPP or FPP. These differences are not surprising because the three RT-ases have different binding constants and maximum reaction rates among the different sizes and stereochemistries of the allylic pyrophosphates (Cornish, 2001a,b).

It has been shown that large APP molecules and their analogs can compete with substrates at the RT-ase binding site(s) (Mau et al., 2003). Also, the large substrate, solanesyl pyrophosphate (SPP), does act as a rubber molecule initiator (Table 1). Thus, it is not unexpected that the benzophenone group on the different BZ substrates did not interfere with rubber molecule initiation. However, similar large substrates do interfere with the activity of UPS, and the crystal structure of microbial UPS enzymes shows large hydrophobic subunits at the end of the protein binding cleft or pocket (Ko et al., 2001; Fujihashi et al., 2001). The RT-ase crystal structure is not known, but biochemical and chemical studies lead to the inference that the active site is cylindrical in form rather than a pocket (Cornish, 2001a,b). This hypothesis is supported by work in which a single amino acid substitution in FPS opened up the floor of the pocket and allowed the mutated FPS to synthesize longer products (Tarshis et al., 1994). The utilization of large substrates by RT-ase for initiation of rubber polymerization, among various other kinetic features, including very high K_m^{IPP}, functionally distinguishes RT-ase from UPS and other CPTs.

The *H. brasiliensis* RT-ase had a stronger affinity (lower K_m) for the large molecular weight Bz-allylic initiators, than for FPP, which was not seen in the *P. argentatum* and *F. elastica* RT-ases. This is similar to their affinities for SPP (Table 1), and explains the ability of the *H. brasiliensis* RT-ase to rapidly incorporate IPP even at the very low concentrations of the large hydrophobic APP initiators utilized here. Thus, the earlier suggestion that rubber biosynthesis by *H. brasiliensis* may occur in two stages, firstly with a *cis*-prenyl transferase producing an allylic pyrophosphate product larger than GPP which then is the true initiator rubber biosynthesis (Wititsuwannakul et al., 2004), is supported by the current study.

RT-ase activity is inhibited when *E,E*-FPP concentrations increase much above those needed to support maximum activity (Cornish, 2001a,b). This normal inhibition of activity makes examination of other inhibitors difficult. Percentage of velocity in FPP has been used as a means to examine chemical inhibitors of FPP initiation (Mau et al., 2003). The inhibitors of FPP binding by protein farnesyltransferases competitively and noncompetitively inhibited RT-ases and this was, again, dependent upon species. Here, we examined the effect of the addition of Bz-GPP(*p*) in presence of *E,E*-FPP to each of the rubber transferases (Fig. 4). The RT-ases of the three species clearly respond differently with respect to effective concentrations and V_{max} (Fig. 12). The maximum velocity for *P. argentatum* still occurred at the same total APP concentration, but both *F. elastica* and *H. brasiliensis* had maximum velocities at lower total APP concentrations. The activation and inhibition slopes of activity from Hill plots (Fig. 12) in *P. argentatum* and *F. elastica* were steeper with the Bz-GPP(*p*) additions compared to FPP alone. In *H. brasiliensis* the activation slope was steeper but the inhibition slope was much less steep, once again indicating that the RT-ases acted quite differently to each other.

Detailed kinetic competition studies of the competitive or noncompetitive nature of these Bz allylic pyrophosphates were not performed. However, the decreased total substrate concentration required for maximum velocity (Fig. 12) in both *F. elastica* and *H. brasiliensis*, suggests that the two substrates may be additive (competitive and noncompetitive) for these two species, but not for *P. argentatum*. It may well be that the benzophenones that had the lowest velocities, Bz-DMAPP(*m*) and Bz-DMAPP(*p*) for *F. elastica*, Bz-FPP(*p*) for *H. brasiliensis*, and Bz-DMAPP(*m*) and Bz-DMAPP(*p*) for *P. argentatum,* are the stronger inhibitors, and may also be useful probes by binding to amino acids involved in initiator binding. As mentioned earlier, the ^{3}H-Bz-GPP (*p*) was selected because of its utility as a good substrate for the RT-ases of all three species.

The addition of EDTA to the reaction did not affect the amount of label accumulated by the rubber particles (Table 2). This finding confirms the kinetic determination that metals are not required for *E,E*-FPP (and other APPs) to interact with the RT-ase active site although they are essential to both IPP binding and to the polymerization reaction (Scott et al., 2003).

The inhibition of *P. argentatum* RT-ase activity in 20 μM E,*E*-FPP and Bz-GPP(*p*) was similar in Bz-GPP(*p*) or *E,E*-FPP alone (Cornish, 2001a,b). However, inhibition of the *F. elastica* and *H. brasiliensis* RT-ases begins at the higher *E,E*-FPP concentrations of 50 μM (Cornish,

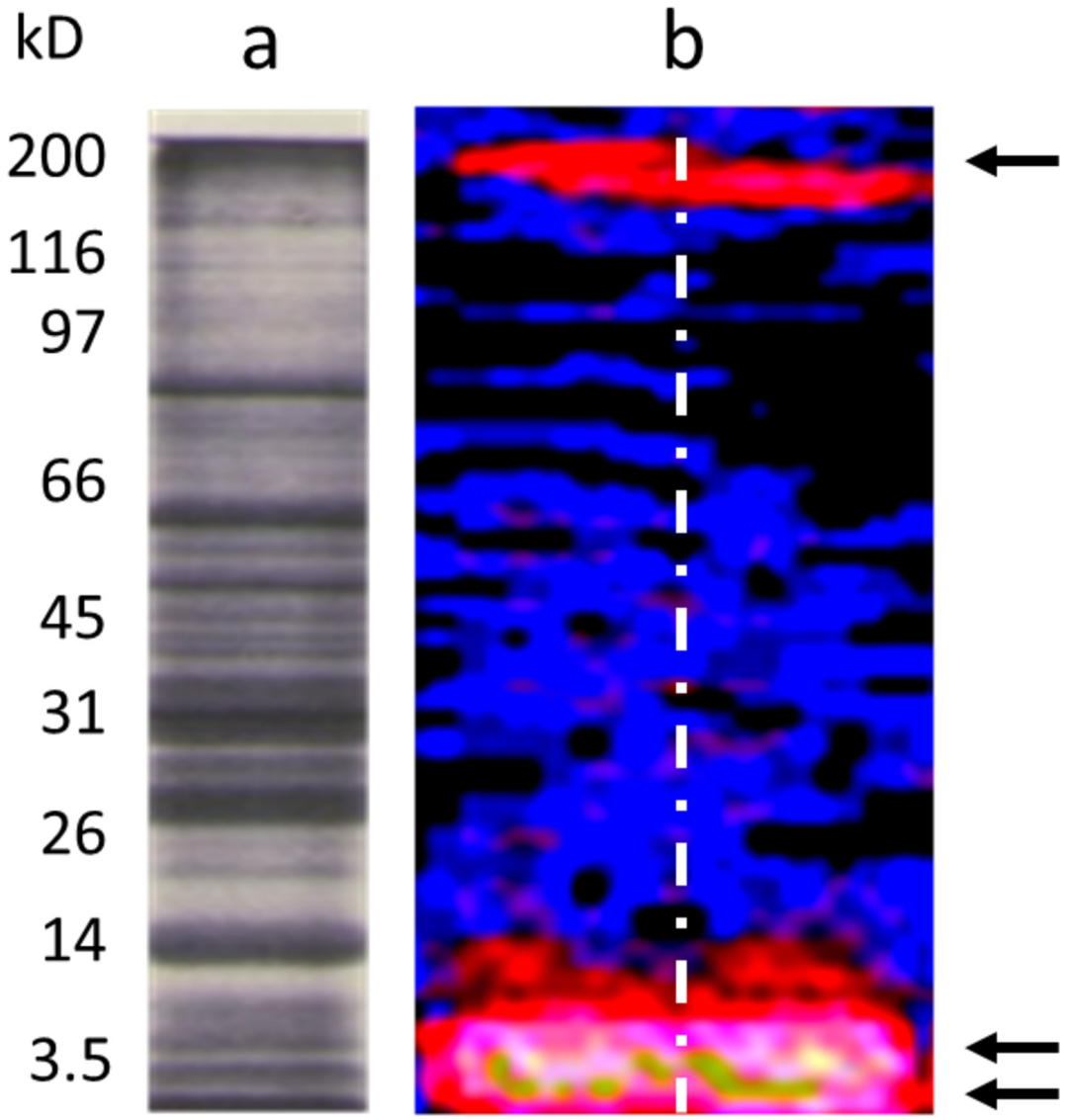

Fig. 5. Enzymatically active rubber particles purified from *Hevea brasiliensis* were exposed to UV light for 90 min in presence of ^{3}H-Bz-GPP, proteins separated by electrophoresis a Bio-Rad 4–20% gradient gel and then scanned for ^{3}H using the Bioscan. Panel a shows one lane of a matched silver stained gel which is sized to match the scan of two lanes shown in panel b (lanes are demarcated by the dashed white line). Labeled proteins in the scan are indicated by the arrows. The broad, low molecular weight, labeled band reflects two distinct small proteins with overlapping tritium alpha particle emissions.

2001b).

A 90% increase in velocity of *H. brasiliensis* RT-ase activity was observed when 10 pM Bz-GPP(*p*) was added to 5 mM E,*E*-FPP. In contrast, 10 pM to 100–100 μM Bz-GPP(*p*) did not affect RT-ase activity in 5 mM E,*E*-FPP in *F. elastica* or *P. argentatum.* Further analysis of the interaction between these two substrates in the three species may be worth additional investigation.

The three RT-ases of all three species contain three very similar proteins which specifically bound detectable photoaffinity labels (Figs. 5 and 6). The rubber particles of all three species contain many more proteins which were not labeled (Figs. 5 and 10). There was stronger labeling of the small proteins than of the large ones. The label found associated with the large proteins appears to be due to their strong association with specifically labeled small proteins rather than to label covalently linked to the large proteins, themselves, because the label on the large proteins diminished when gels were extensively washed, without concomitant loss of label from the small proteins (data not shown). The two covalently labeled small proteins appear to be at the site of APP binding for rubber molecule initiation. This association was confirmed in *P. argentatum* when the large protein was eluted and run on an IEF gel where the pH gradient clearly separated the 1,790 Da and 3,390 Da proteins from the large protein (Fig. 11 b). The interaction of a small protein with a large complex in the biosynthesis of polymers is not unusual for biological systems. In fact it is the method of biosynthesis of fats, utilizing acyl carrier protein (Shanklin and Somerville, 1991). It also has been shown that allylic pyrophosphates can interact, as inhibitors, with the non-allylic IPP binding site of RT-ases (Mau et al., 2003). Thus, it seems possible that the two small subunits may contain both IPP and initiator binding sites because both could probably be labeled by the ^{3}H-BzGPP(*p*).

The pI's of the *F. elastica* and *P. argentatum* large proteins are similar to each other (7.7 and 7.6, respectively. However, the small proteins are very unusual (Table 4). Although they correspond closely in size, the identity of the strongly basic protein is opposite in the two species. The smallest *F. elastica* protein has a pI of 11, but the smallest protein in *P. argentatum* is strongly acidic with a pI of 3.5. The *P. argentatum* 3,990 Da protein has a basic pI of 10.5 but, in *F. elastica*, the similarly sized protein, 3,900 Da, has a pI of 6.0.

The large proteins are proposed to play a structural role, holding the small proteins in an orientation essential for RT-ase active and substrate

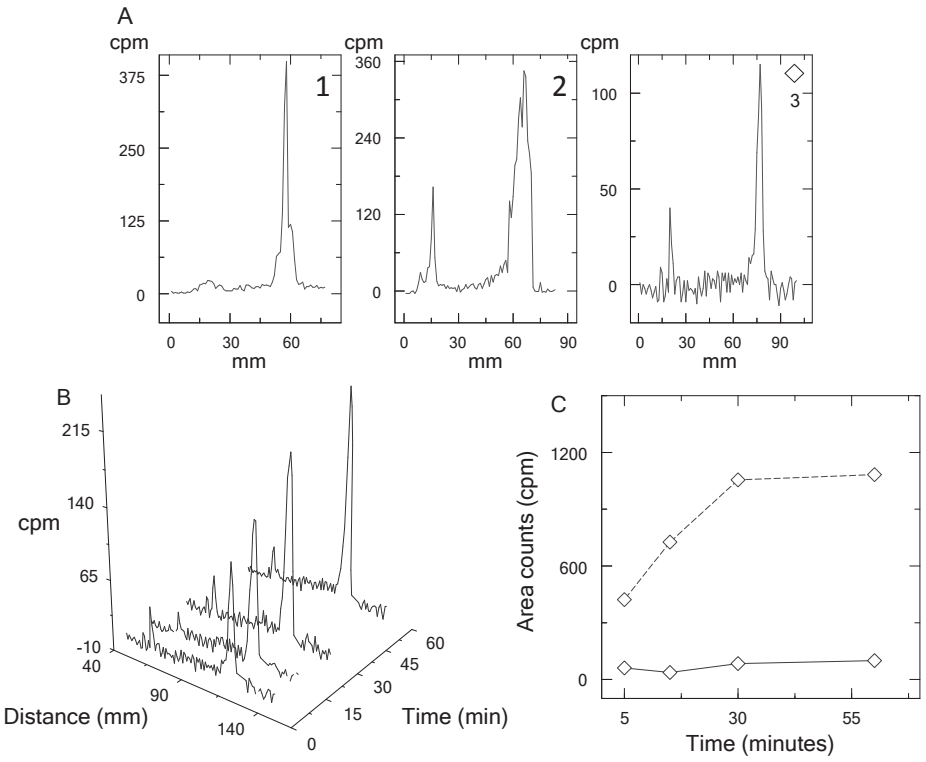

Fig. 6. The effect of UV exposure (5, 15, 30, 60 min) on (A) the accumulation of ^{3}H in photo affinity labeled proteins in 1, *F. elastica*; 2, *H. brasiliensis*; and 3, *P. argentatum P. argentatum*; (B) Winscan 2D analysis of Bioscan chromatograms collected for 90 min on four lanes of a 4–20% polyacrylamide gel of *P. argentatum* proteins; (C) the total ^{3}H cpm incorporated (——) compared to unlabeled proteins (—) from *P. argentatum*.

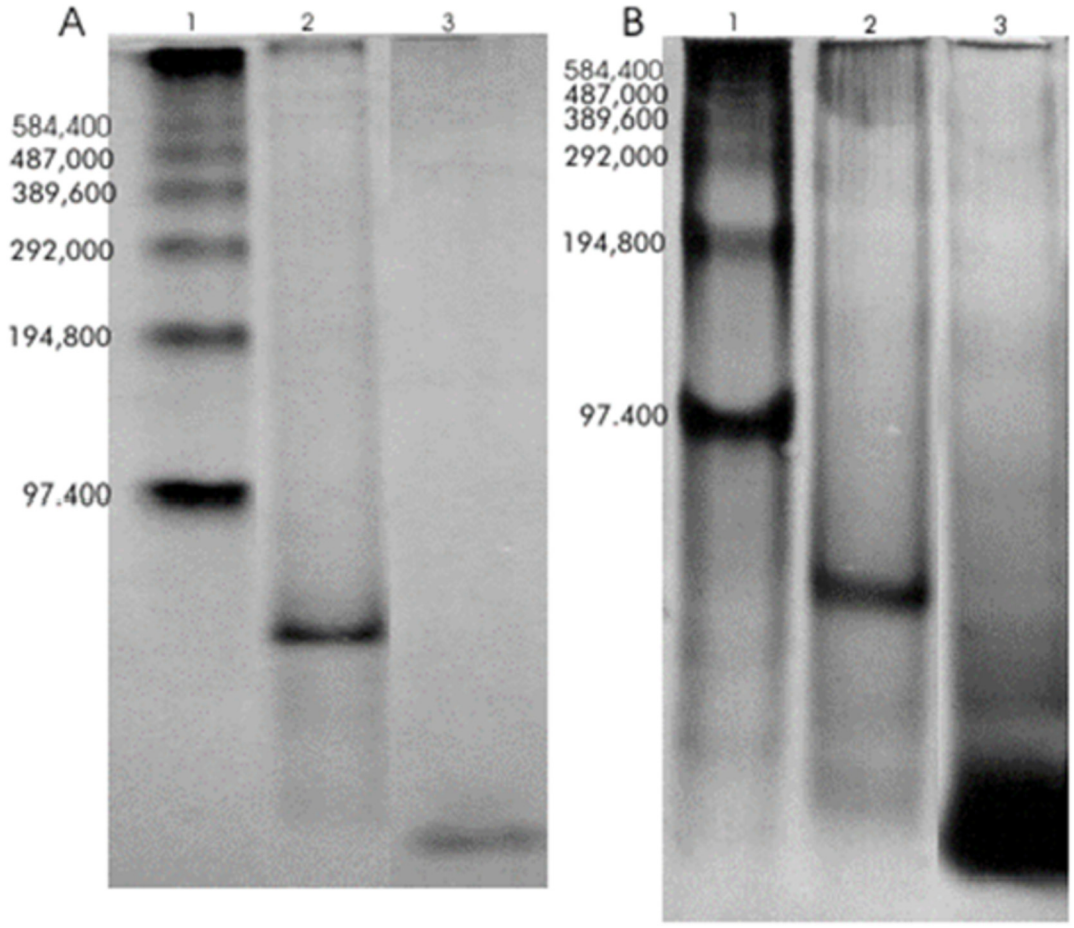

Fig. 7. Photographs of phosphate gels (A, 3.5%; B, 4.0%) used to evaluate the molecular weight of large proteins. Lane 1 contains Sigma cross-linked phosphorylase b standards, lane 2 contains *P. argentatum* (0.2 mg in 10 µl sample buffer) and lane 3 contains *H. brasiliensis* (0.5 mg in 10 µl sample buffer).

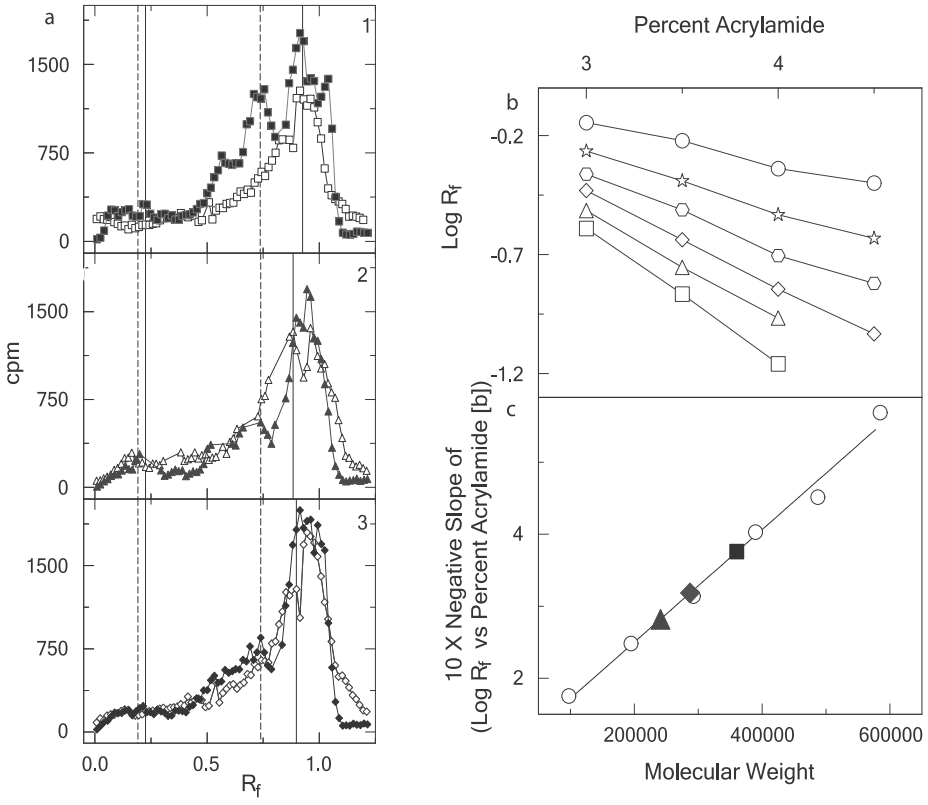

Fig. 8. (a) Radioactivity (cpm) measured by 8 h Bioscans of 4% (open symbols) and 4.5% (filled symbols) polyacrylamide gels versus R_f for (1) *F. elastica*, (2) *H. brasiliensis* and (3) *P. argentatum*. The two lefter most vertical lines represent R_f's of a 200,000 Da standard on a 4.0% (—), and 4.5% (———) gel, and are 0.227 and 0.192, respectively. The two righter most vertical lines reflect the R_f's of a smaller standard protein run on 4 and 4.5% gels with (1) *F. elastica*, (0.925, 0.736) for (2) *H. brasiliensis* (0.883, 0.739) and (3) *P. argentatum* (0.898, 0.739). (b) Percent acrylamide versus log R_f of phosphorylase b polymers ○ 97,000; ☆194,800, ⬡ 242,000; ◇ 389,600; △ 487,000; □ 584,400. (c) Negative slope (times 10) of Log R_f plotted against molecular weight. ○ Standards, ■ *F. elastica* (3.88, 375,000), ▲ *H. brasiliensis* (2.62, 287,000), ◆ *P. argentatum* (3.18, 215,000). Equation for standard line: y = 0.00000782x + 0.9371.

binding. However, in spite of this functional similarity, the large protein in *F. elastica* is a 360,000 Da monomer (Siler and Cornish, 1993) but in *P. argentatum* appears to be largely assembled from four or five 52,000 Da subunits (RPP) (Siler and Cornish, 1994). The *P. argentatum* protein associated with the large molecular weight protein separated by IEF with a pI of 6.3 is most likely the RPP protein, 52,000 Da, pI 6.1 (Backhaus et al., 1991), which was identified as a cytochrome P450 oxide synthase (Pan et al., 1995). However, no label was associated with proteins of this size either with or without strong denaturants, indicating a more indirect role in RT-ase activity than substrate binding. Cytochrome P450 oxide synthases are involved in prenyl transferase reactions by transferring electrons. This suggests that RPP may serve both as a key structural component of the complex and as the source of electrons essential during the large energy release that occurs as the pyrophosphate is cleaved during the condensation reaction of IPP and the elongating APP end of the elongating rubber polymer.

Ferguson analysis (Ferguson, 1964) of the proteins separated by the phosphate polyacrylamide gels demonstrated that the molecular weight of the rubber particle large proteins, given by the slope of the plot (Fig 8b, c) was much greater than suggested by the simple mobility of the proteins in the gels (Fig. 7), and which assumes, incorrectly, an equal charge density for all SDS-proteins (Rodbard & Chrambach, 1970, 1971). This difference is exacerbated by glycosylation of some rubber particle proteins but not others ((Backhaus et al., 1991; Siler and Cornish, 1993). The *P. argentatum* 287,000 Da protein ran toward the bottom of the 3.5% and 4% gels (Fig. 7A and B, lane 2), as did the *H. brasiliensis* 214,000 Da protein (Fig. 7A and B, lane 3). The standards (Fig. 7A and B, lane 1) migrated much less far into the gel and even the 90,000 Da protein standard migrated a shorter distance than the two large rubber particle proteins. This is very common for glycoproteins and makes Ferguson analysis much more important in order to accurately determine protein size. Migration was less of a problem on the Novex gradient gels (Fig. 11 a) where the standards more accurately matched the molecular weight of the rubber particle glycoproteins.

The slopes of the Hill plots for *E,E*-FPP and FPP + Bz-GPP (*p*) (Fig. 12) indicate that the number of substrates required to activate the enzymatic activity was maximally three and the subunit ratios between the small subunits and the large subunit also were around three (Table 6). This number match is additional evidence that the small proteins are the site of allylic pyrophosphate substrate binding. This was also supported by the non-dilutive label associated with the small proteins, but not with the large ones when the gels were washed. Thus, the small proteins had covalently bound the labels, but the decline in the label associated with the large protein suggests that these are a scaffold of some kind which tightly, but non-covalently, holds onto the small proteins. The native large protein in *F. elastica* (Siler and Cornish, 1993) is a dimer of the 360 kD monomer (thought to be 376 kD at that time) (Siler and Cornish, 1994). This suggests that there are six of the small proteins and two of the large proteins associated with each native RT-ase complex. Their potential as binding site subunits is also supported by a model of the smallest *F. elastica* protein for which the amino acid sequence has been determined (unpublished results). The minimized 3-D structure of this protein is compatible with both FPP and IPP binding (Fig. 13). This hypothesis may or may not prove to be true, of course.

The concept of, and justification for, a RT-ase pore through the rubber particle membrane has previously been described (Cornish, 2001a,b, Cornish et al., 1999). Substrate binding without additional elongation (*P. argentatum* RT-ase activity was inhibited by 5 min of UV in Bz-GPP(*p*) (Fig. 3) while APP incorporation continued, supports this concept if the RT-ase were a cylindrical pore with several small proteins available for initiating rubber transferase activity, as indicated above (see schema in Fig. 14). Since the pore size of the RT-ase is relatively small, the initiating benzophenone protein (which is larger than the size of the substrate interactive region available in P. *argentatum*), once covalently linked to the complex, would block the progression down the pore, but would not block the ability of the other small proteins to bind initiator from the cytosol until all sites are initiated. This seems to occur in all three RT-ases even though the *F. elastica* 360,000 protein is an integral membrane protein that traverses the rubber particle

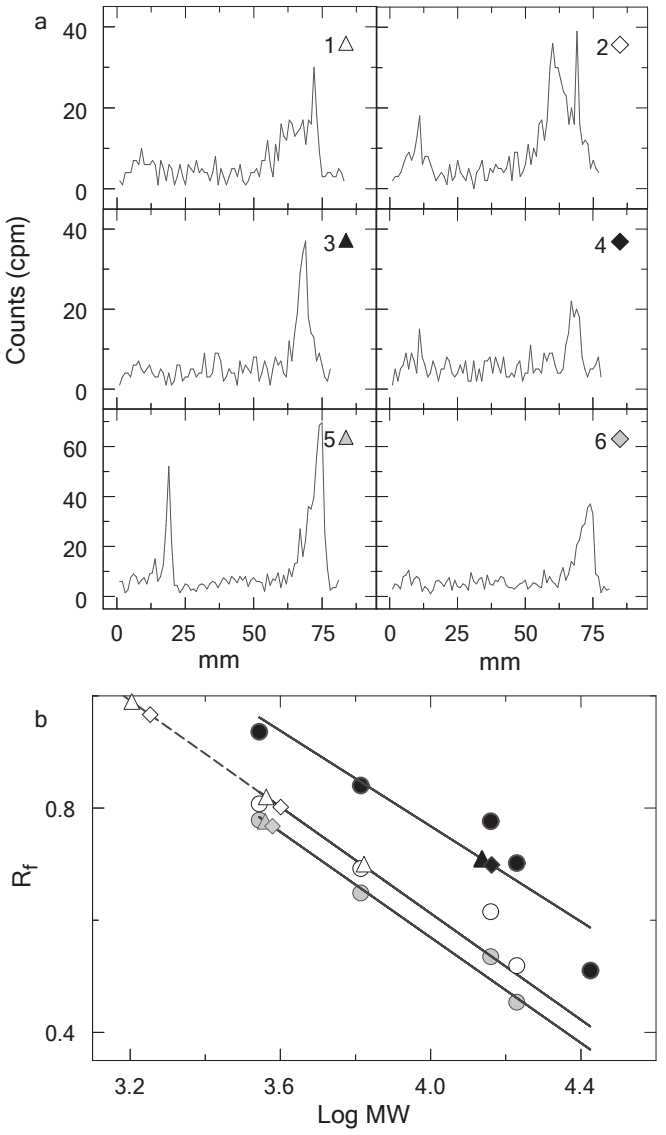

Fig. 9. (a) Bioscan chromatograms of 18% (open symbols), 15% (black symbols) and 16.5% (gray symbols) gels. *H. brasiliensis* labeled proteins are shown in 1 (18%), 3 (15%), and 5 (16.5%) whereas *P. argentatum* labeled proteins are shown in 2 (18%), 4 (15%), and 6 (16.5%). (b) R_f versus Log MW. (▬) Standard curve on an 18% Tris-HCl gel with Δ *H. brasiliensis* and ◇ *P. argentatum* proteins. Equation for the line is $y = -0.4746x + 2.5104$. (—) Standard curve on a 16.5% Tris-Tricine gel with △ *H. brasiliensis* and ◇ *P. argentatum* proteins. Equation for the line is $y = -0.4702x + 2.4502$. (▬) Standard curve on 15% Tris-HCl gel with ▲ *H. brasiliensis* and ◆ *P. argentatum* proteins. Equation for the line is $y = -0.4252x + 2.4685$. The standards Bio-Rad 326 protein sizes shown as circles expressed in Daltons and ($\log_{10}$ MW) are: 26,625 (4.42529); 16,950 (4.22917); 14,437 (4.159477); 6512 (3.813714); and 3496 (3.543571).

biomembrane into the particle interior, whereas the *P. argentatum* and *H. brasiliensis* large proteins are positioned at the particle surface and do not appear to penetrate beyond the depth of the membrane into the particle interior (Cornish et al., 1999).

The overall architectural and three dimensional structural features of the RT-ase complexes are clearly conserved across species, including the remarkable similarly in size of the three subunits reported here and the surface epitopes of the proteins. Proteins from purified rubber particles of *F. elastica*, *H. brasiliensis* and *P. argentatum* specifically bound polyclonal antibodies raised against *P. argentatum* rubber particles, including the 1,900, the 3,900 and 306,000 Da F. *elastica,* the

Table 4
Molecular and biochemical characteristics of rubber particle proteins specifically labeled by ^{3}H-Bz-GPP(*p*).

Species	Molecular Weight (*Da*)	pI	Predicted amino acid number[c]	Predicted base pair number[d] for mature mRNA
Ficus elastica	360,000	7.7[a]	3006 (3050)[b]	9017
	3900	6.0[e]	36	108
	1800	11.0[e]	16	48
Hevea brasiliensis	241,000	n.d.	2012	6036
	3650	n.d.	30	91
	1600	n.d.	13	40
Parthenium argentatum	287,000	7.6	2396	7188
	3990	10.4[e]	33	100
	1790	3.5	15	45

n.d. Not determined.

[a] Calculated using Protein Sequence Analysis Shareware Version 1.2 by Ira W. Palmer on http://iubio.bio.indiana.edu/soft/molbio/Listings.html Archive iubio/ibmpc/prot-sa* based on amino acid composition found listed in (Siler and Cornish, 1993).

[b] Number of amino acid residues found in (Siler and Cornish, 1993).

[c] Calculated with the assumption that average amino acid is 119.78 Da.

[d] Calculated with the assumption that three base pairs associated to each amino acid in the mature mRNA. (Not including the stop codon.)

[e] Calculated using ExPASy https://web.expasy.org/cgi-bin/compute_pi/pi_tool.

3,700 and 260,00 Da *P. argentatum* proteins, and a protein approximately 14,000 Da from *H. brasiliensis* (D.J. Siler unpublished data). Also, polyclonal antibodies raised against the large *F. elastica* protein strongly reacted with *F. elastica* and *P. argentatum* WRP dot blots but less strongly with *H. brasiliensis* WRP (Siler and Cornish, 1993). It is interesting that the structural conservation of the RT-ase complex holds, even though particle size, and the flexibility of the rubber particle biomembrane does not. *F. elastica* particles are large, and their uni-biomembrane is rigid, containing integral proteins and waxy fatty acids. This strongly contrasts with the flexible uni-biomembranes of the smaller *H. brasiliensis* and *P. argentatum* rubber particles, which have non-waxy fatty acids and little integral protein (Cornish et al., 1999; Siler et al., 1997). However, these features are clearly unrelated to rubber biosynthesis, *per se*.

This study represents the use of benzophenone photolabels in the largest supramolecular assembly to date (Dorman et al., 2016). The photoaffinity labels also allow estimation of the number of binding sites per rubber particle, which range from 2,000 to 140,000 depending on the species and reaction (Table 2). Assuming that each RT-ase can synthesize six rubber molecules simultaneously, this indicates a maximum number of RT-ase complexes of 23,333 per particle. However, the WRP used consisted of all the rubber particles which could be extracted, included those sequestered by the vacuoles, which are likely to be enzymatically-inactive and may not be competent to bind the Bz-GPP(*p*) substrate. This is supported by calculations based on the size of the large proteins, assuming that they are globular, and that each RT-ase complex contains two large proteins. Using the mean particle diameters of 3.7, 1.4 and 1.0 μm for *F. elastica*, *P. argentatum* and *H. brasiliensis*, respectively, the maximum numbers of RT-ase complexes per rubber particle that can fit within the available surface area are approximately 1,000,000, 155,000 and 84,000 for *F. elastica*, *P. argentatum* and *H. brasiliensis*, respectively, much larger numbers than the labeled complexes. Also, there are many other rubber particle bound proteins which, presumably, would intersperse the RT-ase complexes, even if all particles were enzymatically-active.

This paper does not suggest that the findings of other researchers are incorrect, simply that they are incomplete, and that no single report has elucidated the structure of a functional RT-ase complex and how the different components of such complexes regulate activity and molecular weight. SRPP (23,000 Da), and possibly REF (14,600 Da) appear to play

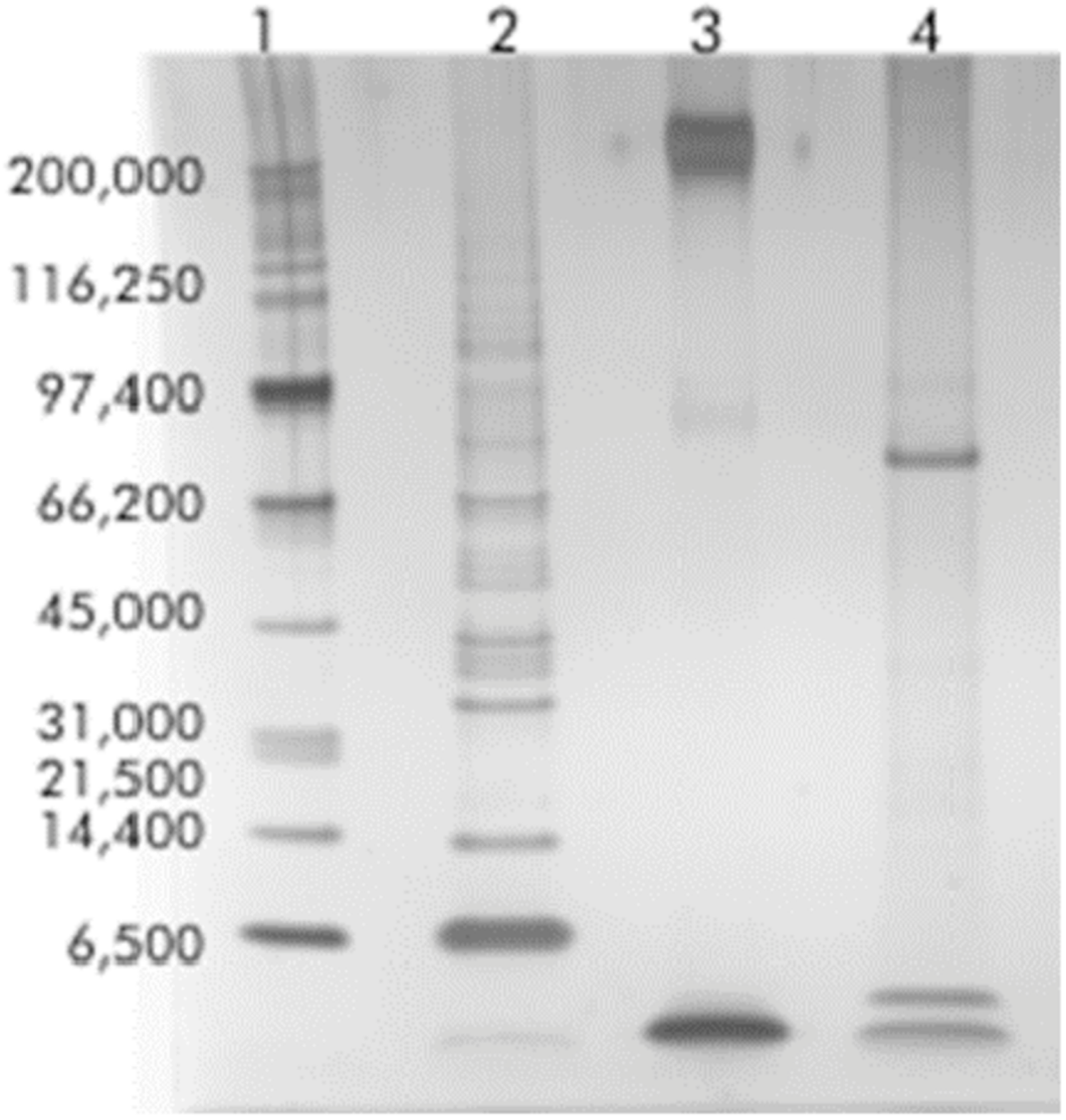

Fig. 10. Comparison of silver stained proteins from rubber particles run on a 12% NuPAGE Novex Bis-Tris gel with Bio-Rad Broad range standards (lane 1), *H. brasiliensis* (lane 2), *F. elastica* (lane 3) and *P. argentatum* (lane 4).

a role in molecular weight regulation in *H. brasiliensis, Taraxacum koksaghyz* and perhaps *P. argentatum* (which has an SRPP homolog) (Collins-Silva et al., 2012; Schmidt et al., 2010a), and the *H. brasiliensis* HRT-1 (33,000 Da), but not HRT-2, is able to restore RT-ase activity to partially deproteinized rubber particles (Yamashita et al., 2016). However, none of these proteins was labeled in this current study, suggesting their lack of direct involvement in substrate binding in rubber biosynthesis.

4. Conclusions

We have identified one large and two very small rubber particle proteins which are directly involved in binding the substrates into the active site of three phylogenetically distant rubber-producing species. The large protein is membrane bound whereas the two small proteins are strongly associated with the large proteins but not the rubber particle biomembrane. The exact role of the small proteins as possible substrate chaperones, activators or binding sites in the RT-ase reaction, and their relationship to, and interactions with, other proteins believed to be part of the RT-ase transferase enzyme complex will only be fully understood when RT-ase crystallography in the presence of different substrates and cofactors is achieved.

5. Experimental

5.1. Plant materials

Mature, field-grown *P. argentatum* (line 11591) (Heliantheae tribe of the Asteraceae) plants were grown at the US Water Conservation Laboratory, Phoenix, AZ, and shipped, on ice, to the USDA-ARS Western Regional Research Center, Albany, California. *F. elastica* (Ficeae tribe of the Moraceae) plants were purchased from a local nursery and grown in a greenhouse at Western Regional Research Center. Freshly tapped, living latex from *H. brasiliensis* (Micrandeae tribe of the Euphorbiaceae) line PB260 was donated by the Rubber Research Institute of India, and shipped on ice to Western Regional Research Center.

5.2. Chemicals

Unlabeled IPP, *E,E*-FPP (*trans,trans*-FPP), and [^{14}C]IPP (55 mCi/mmol) were purchased from American Radiolabeled Chemicals Inc., St. Louis, MO, USA. Benzophenone substituted APPs (Fig. 1a.), benzophenone dimethyl pyrophosphate *para* (Bz-DMAPP (*p*)), benzophenone dimethyl pyrophosphate *meta* (Bz-DMAPP (*m*)), benzophenone geranyl

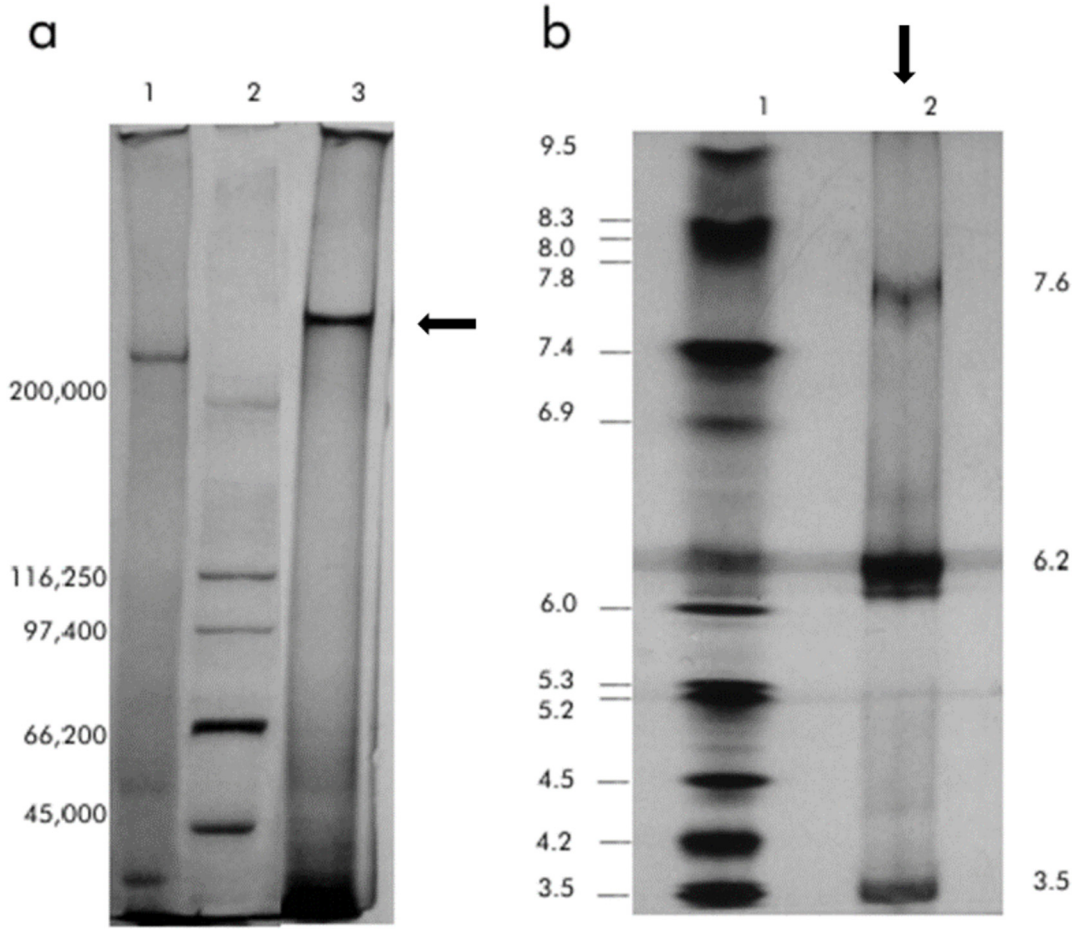

Fig. 11. (a) Novex 3–8% Tri-Acetate gel: lane 1, *H. brasiliensis*; lane 2, molecular weight standards; lane 3, *P. argentatum* proteins 280,000 Da protein band indicated by arrow. (b) Novex 5% IEF gel: lane 1, IEF standards; lane 2, 280,000 Da protein from gel (a) lane 3 was electroeluted and concentrated before loading on the gel. IEF standards are as described in the methods.

pyrophosphate *para* (Bz-GPP (*p*)), and benzophenone-farnesyl pyrophosphate *meta* (Bz-FPP (*m*)), and 150 nmol/ml ^{3}H-BzGPP(*p*) with specific activities of 25–250 mCi/mmol (0.01%–0.1% labeled) were synthesized by Yi Feng Zheng by the method of Marecak (Marecak et al., 1997) and generously donated by Professor Glenn Prestwich, University of Utah, Salt Lake, Utah. Solanesyl pyrophosphate (SPP) was purchased from Sigma (St, Louis, MO, USA). Siliconized 1.5 ml microfuge tubes were purchased from USA, Scientific (Ocala, FL, USA). Ready Safe scintillation fluid was purchased from Beckman Instruments, Fullerton, CA, USA. All other chemicals, unless noted otherwise, were purchased from Sigma (St. Louis, MO, USA).

5.3. Purified, washed, rubber particles

Enzymatically-active RPs were purified as described from *H. brasiliensis* (Cornish, 1993) and *P. argentatum* (Cornish and Backhaus, 1990) (WRP, washed rubber particles). Enzymatically-active, buoyant, WRPs of *F. elastica* were collected and purified from latex tapped from stems and petioles of mature plants, collected on ice into buffer containing 1.25 mM $MgSO_4$ and 100 mM Tris-HCl, pH 7.5, and purified by centrifugation as described previously (Cornish and Siler, 1996). The purified WRP of all three species were stored at −80 °C, after being adjusted to 10% glycerol and flash frozen as droplets in liquid nitrogen (Cornish and Bartlett, 1997).

Table 5
The percentage of label incorporated by the different subunits was calculated for *H. brasiliensis* and *P. argentatum*. The apparent molecular weights of the small proteins are affects by gel concentration (% acrylamide).

Species	Large Protein			Small Protein			Smallest		Protein
	4%	4.5%	4–20%	15%	16.5%	18%	15%	16.5%	18%
Hevea brasiliensis									
Molecular Weight	241,000	241,000		13.7	3.79	3.98	13.7		
% Counts[a]	0.21	0.20	0.25	0.62	0.58	0.25	0.62		
Parthenium argentatum									
Molecular Weight	287,00	287,000		14.1	3.63	2.89	14.1		
% Counts[a]	0.25	0.31	0.17	0.75	0.38	0.67	0.75		

[a] Tritium accumulation rate (36 cpm/0.06 µl) for 10 µM ^{3}H-Bz-GPP(*p*) was similar to the tritium counted in scintillation vials around (44 cpm/0.06 µl). Therefore, we calculated the percentage of the counts per peak (area under the curve in cpm) divided by the total cpm in the sample loaded onto the gel. The 18% data are the means of 2 and 3 determinations for *P. argentatum* and *H. brasiliensis*, respectively.

Table 6
Ratio of labeled protein number to number of large proteins in two species. The mean of the two largest % counts in Table 5 for each smaller and smallest protein were expressed as a ratio of the counts in the large protein for each species.

Species	Protein type	
	Smaller	Smallest
	(*Ratio against number of large proteins*)	
Hevea brasiliensis	2.72	2.82
Parthenium argentatum	2.92	3.08

Calculated as the mean of the two highest % counts in Table 5, for each smaller and smallest protein, expressed as a ratio of the mean counts in the large protein for each species.

Table 7
Activation (n_{app}) by allylic pyrophosphate substrates for three rubber transferases were calculated from Hill plots (Fig. 12a for FPP, Hill plot of SPP not shown).

Species	Maximum n_{app}	
	Allylic pyrophosphate	
	FPP (C_{15})	SPP (C_{45})
Ficus elastica	1.2	0.8
Hevea brasiliensis	2.2	3.6
Parthenium argentatum	2.6	2.4

5.4. Rubber transferase activity assays

RT-ase activity in WRPs from *P. argentatum F. elastica*, and *H. brasiliensis* was measured in low retention (siliconized) 1.5 ml microfuge tubes, as described previously (Cornish and Backhaus, 1990; Espy et al., 2006; Cornish, 1993). Routinely, 1 mg of WRP (dry weight basis) were assayed with various concentrations of APP initiators, 5 mM IPP (a nonlimiting monomer concentration), and wash buffer (WB) (1.75 mM $MgSO_4$, 50 µM dithiothreitol (DTT), 100 mM Tris-HCl, pH 7.5, 1 mM pefabloc). The APPs were *E,E*-FPP, solanesyl pyrophosphate (SPP), and four benzophenone-substituted APPs: Bz-DMAPP (*p*), Bz-DMAPP (*m*), Bz-*E*-GPP (*p*), and Bz-*E,E*-FPP (*m*). When the APP initiator SPP was used as a substrate, 0.08% CHAPS (3-[(3-cholamidopropyl) dimethylammonio]-1-propanesulfonate) was added to the reaction mixture to improve solubility of this large substrate. *H. brasiliensis* and *F. elastica* WRPS were incubated for 4 h at 25 °C and *P. argentatum* WRPs for 4 h at 16 °C in RTE-100 NesLab water baths. The conditions support linear substrate accumulation rates throughout the reaction period. Also, less than 1% of APP and IPP substrates were polymerized in rubber polymers during these assays. The reactions were halted by the addition of 25 mM EDTA and the rubber was collected by filtration onto 0.45 µm filters, dried, weighed, washed once with 3 mls of 1 M HCl, twice with 3 mls of 95% ethanol, and then placed in 10 ml scintillation vials containing 5 mls scintillation fluid. The incorporated ^{14}C-IPP was quantified using a liquid scintillation counter (Beckman LS6500).

Covered tissue culture plates (Falcon 3705) were used to determine the RT-ase activity remaining after UV light exposure, of 1 mg–12 mg of WRP using the plate assay method and a 50 µl reaction mix (Mau et al., 2000). The plates were siliconized with Sigmacote (Sigma-Aldrich, Corp., St. Louis, MO, USA, #SL-2) for 2 min, rinsed with ddH_20, then with 95% ethanol, and dried overnight at room temperature. For each reaction, the 50 µl reaction mix contained 5 mM IPP (^{14}C IPP: routinely 150,000 dpm/reaction), WB, and, when present, 5 mM E,*E*-FPP and/or 25 mM EDTA. The plates were placed in the dark for 4 h on a cooling plate (Amersham Pharmacia Cooling Plate #18-1103-46 (210 × 270 mm)) attached to a water bath (RTE-100 NesLab), one set at 25 °C for *H. brasiliensis* and *F. elastica* WRP and one set at 16 °C for *P. argentatum* WRP, both with slow rotation (Gyrotory shaker Model G-2, New Brunswick Scientific Company, Inc., Edison, NJ). After pipetting the reaction mixtures from the wells onto filters, the labeled rubber was filtered, dried, weighed, washed and radioactivity determined by liquid scintillation spectroscopy.

5.5. Photo affinity labeling

5.5.1. Construction of the light shelf

A light shelf was constructed as described (Marecak et al., 1997) with the following modifications. Ten lamp holders (#RPR) were attached to a painted wooden shelf (13 × 32 × 64 cm). The lamps were placed in parallel so that the UV 350 nm lamps (#RPR3500) illuminated the center of five rows of two 96 well tissue culture plates, *i.e.* three lights, each light to illuminate rows B, E, and G of one plate, and two lights, each light to illuminate rows B and E of the second plate. The transformers (#SS-2) and an AC surge protector equipped with five individual switches were attached to the other side of the shelf. Items #RPR, #RPR3500 and #SS-2 were purchased from Southern New England Ultraviolet Company, 550-29 East Main Street, Branford, CT 06405, USA. A bubble leveler was added to the shelf. Two large laboratory jacks were used to raise and lower the light apparatus. Illuminations were carried out with the lamps set at a maximum distance from the plates of 0.3 cm.

5.5.2. Photo affinity labeling of rubber particle proteins

Reactions were performed in individual wells of siliconized 96-well flat bottom tissue culture plates (Falcon 3705). Reactions (total volume of 25 µl) contained WRP (1–2 mg), 10 pM to 45 µM of either Bz-DMAPP (*p*) or Bz-GPP(*p*) and WB. The reaction mixture in each cell was thoroughly mixed by repeated pipetting. Plates were placed under the lamps on a leveled cooling plate set and equilibrated to 4 °C. Care was taken to ensure that each lamp was centered over the appropriate well

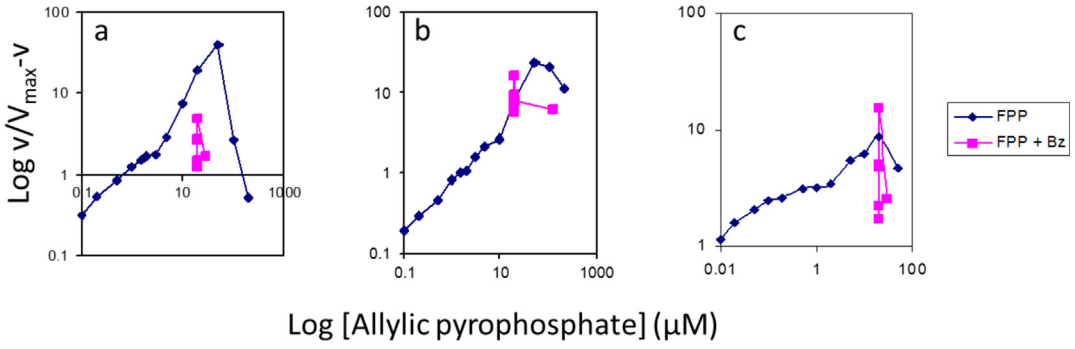

Fig. 12. Hill plots of IPP incorporation rate as a function of allylic pyrophosphate concentration in the *E,E*-FPP alone (♦) or with *E,E*-FPP and Bz-GPP (▲), for (a) *H. brasiliensis*, (b) *F. elastica* and (c) *P. argentatum*. The intercept at y = 1 is the K_m^{IPP}.

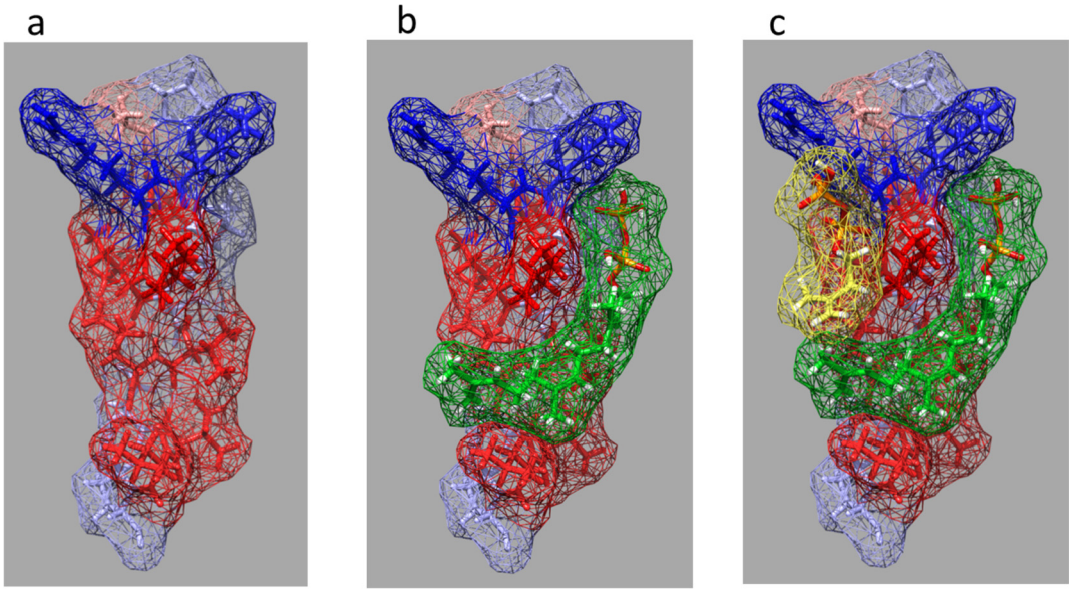

Fig. 13. Predicted minimized folded molecular structure, from the amino acid sequence (not shown), of the 1,800 Da protein from *F. elastica* rubber particles. (a) The peptide backbone, colored by amino acid hydrophobicity (red, high; blue, low); (b) with FPP (by atom, backbone in green) and (c) with FPP and IPP (by atom, IPP backbone in yellow). The model was created using Pymol v1.7.

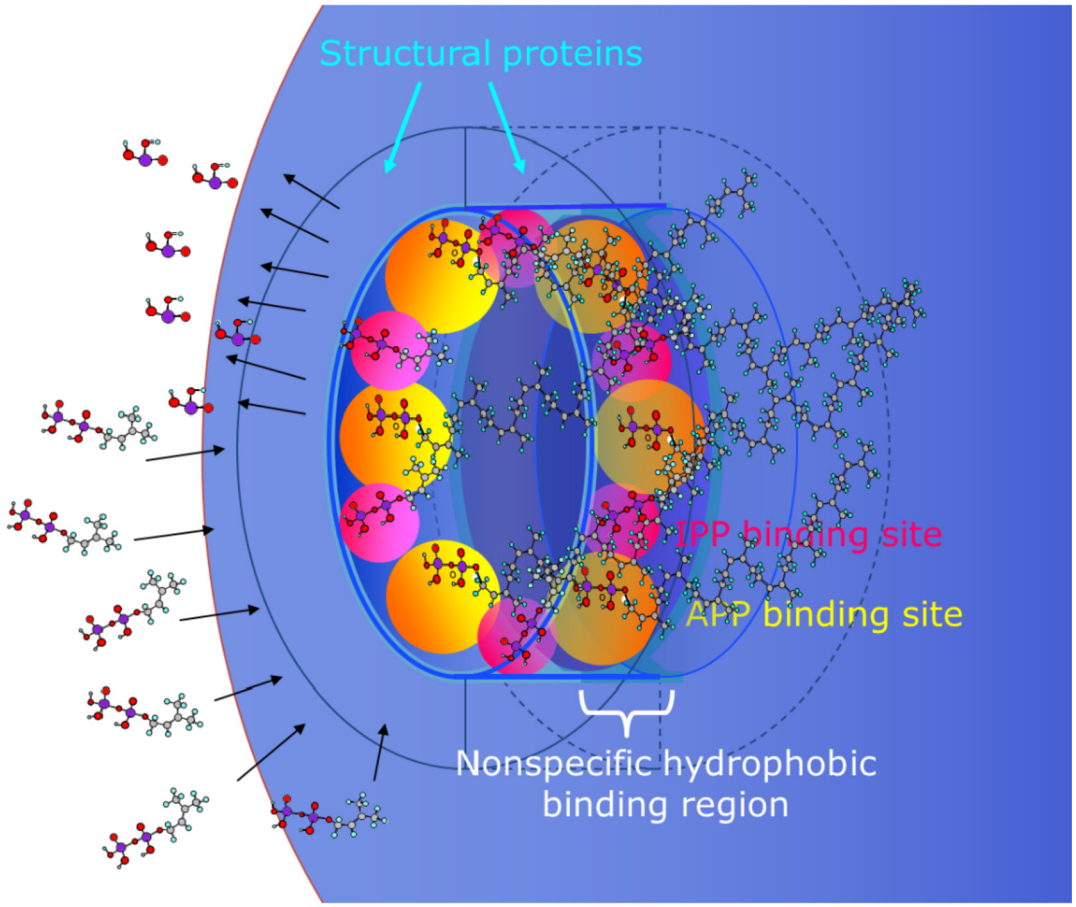

Fig. 14. A schema of the RT-ase illustrating the proposed dimeric large protein and three each of the two small proteins (not drawn to scale) and the pore traversing the membrane to the particle interior. The hydrophobic FPP and IPP substrates bind to the catalytic site and phosphate is released at each condensation step. The rubber molecule interacts with a non-specific hydrophobic binding region until it reached the particle interior. The binding sites are labeled pairing protein and substrate size, but this may not be correct.

row, as described above. The lamp shelf was then lowered to 0.3 cm and the bubbler used to ensure that the shelf (and plate) was level.

5.5.3. Inhibition of rubber transferase activity by UV light exposure

When all the reactions were to be exposed to UV light for the same period of time, the samples were either assayed as described above, or stored for analysis by gel electrophoresis at −20 °C in various sample buffers, as described below. However, when more than one time period was to be compared, the reactions were staggered to permit appropriate exposures. For example, for an experiment with 30 and 60 min UV light exposure, WRP and reaction mix were added to row B on plate 1. The light above row B was turned on for 30 min; then more purified rubber particles and Bz-APP initiator in reaction mix were added to row E, and the lights for row B and row E also were turned on for 30 min. Thus, the total time of light exposure for row B was 60 min and for row E was 30 min. This method was extended for light exposures of 60, 30, 15, and 5 min. WRP were kept on ice until pipetted into the reaction plate.

5.5.3.1. Ficus elastica. For each reaction, 1 mg of WRP was suspended in 40 µl of WB containing either 50 µM Bz-GPP(*p*) (the concentration reference for 50 µl assay volume) or no APP. After UV light exposure, the volume was adjusted to 50 µl and final concentrations of 20 µM E,*E*-FPP, 5 mM IPP (^{14}C-IPP, 128,220 dpm), both non-limiting concentrations. For each time point, assays were performed in duplicates of 50 µM Bz-GPP(*p*), one of 20 µM E,*E*-FPP and one assay without an APP initiator. For the zero time point (no UV exposure) assays were performed in duplicates of 50 µM Bz-GPP(*p*), duplicates of 20 µM E,*E*-FPP, one of 20 µM E,*E*-FPP with 20 mM EDTA, and one reaction without APP initiator.

5.5.3.2. Hevea brasiliensis. For each reaction, 1 mg of WRP was suspended in 40 µl of WB containing 20 µM E,*E*-FPP, 10 µM Bz-GPP(*p*) or 4 µM Bz-DMAPP (*p*) (the concentration reference for the 50 µl assay volume). After UV light exposure, the volume was adjusted to 50 µl and a final concentration of 5 mM IPP (^{14}C-IPP, 106,027 dpm). For each time point, assays were performed in triplicate reactions of 20 µM E,*E*-FPP, one of 4 µM Bz-DMAPP(*p*), one of 10 µM Bz-GPP(*p*) and one 20 µM E,*E*-FPP with 20 mM EDTA as a control.

5.5.3.3. Parthenium argentatum. For each reaction, 0.75 mg of WRP was suspended in 40 µl of WB containing 10 µM Bz-GPP(*p*) (the concentration reference for the 50 µl assay volume) or no APP. After UV light exposure, the volume was adjusted to 50 µl for a final concentration of 20 µM E,*E*-FPP, and 80 µM IPP (^{14}C-IPP, 102,247 dpm) (a limiting IPP concentration). For each time point, assays were performed in duplicates of 20 µM E,*E*-FPP, triplicates of 10 µM Bz-GPP (*p*), and a single reaction of 20 µM E,*E*-FPP with 20 mM EDTA as the control.

5.5.4. Verification of adequate labeling

Validation of adequate labeling of the proteins on WRP using the described methods was confirmed using *H. brasiliensis* WRP. Samples containing 1 mg WRP were added to each of 18 wells of a tissue culture plate. Each well contained 25 µl of 50 µM, 10 µM or 1 µM of ^{3}H-Bz-GPP (*p*) with and without 25 mM EDTA, assayed in triplicate. After 60 min exposure to UV at 4 °C, the contents of each well were pipetted onto a filter inside a scintillation vial and dried for one hour at 37 °C. The filters were washed first with 3 ml 1 M HCl, and then repeatedly washed up to 22 times with 3 ml 95% ethanol. Each wash was individually transferred to a 15 ml scintillation fluid and counted for ^{3}H using a Beckman scintillation counter, model LS6500. When the counts found in the wash were at background for two consecutive washes, the counts remaining on the filter were quantified.

An additional eight wells of the same tissue culture plate were set up for RT-ase activity assays. Four wells, each containing 1 mg WRP and either 50 µM Bz-GPP(*p*) or 20 µM E,*E*-FPP, with and without 25 mM EDTA, were exposed to 60 min of UV light at 4 °C with mixing as described above. After the samples exposed to UV light were transferred, four additional wells were set up. To each of these eight wells an additional 25 µl were added to make 20 µM E,*E*-FPP, 5 mM IPP (^{14}C-IPP 140,000 dpm), and 1.25 mM $MgCl_2$. These were incubated for 4 h at 25 °C to determine RT-ase activity.

5.5.5. The effect of UV light exposure on tritiation of rubber particle-bound proteins

To determine a suitable UV exposure time for maximal labeling, 3 mg of *P. argentatum* WRP, 50 µM ^{3}H-Bz-GPP(*p*) and WB for each 50 µl reaction mixture were placed in wells of a falcon tissue culture plate. After UV exposure times of 5, 15, 30, and 60 min, the contents of each well were transferred to siliconized microfuge tubes to which 17 µl of 4× white sample buffer (WSB: 0.125 M Tris-HCl, pH 6.8, 4% sodium dodecyl sulfate (SDS), 40% glycerol, 2.85 M 2-mercaptoethanol) were added, heated at 95 °C for 5 min, and stored at −20 °C. The protein samples were separated by electrophoresis on 4–20% polyacrylamide gels (Bio-Rad, Hercules, CA) run at 100 V for 90 min, and scanned for incorporated tritium using a Bioscan 200 Imaging Scanner. Similar experiments were performed using 10 mg/well *H. brasiliensis* WRP particles and 1 mg/well *F. elastica* WRP. Note: WSB was used because the Bromophenol Blue stain in blue sample buffer (BSB) co-eluted with small proteins of interest.

5.5.6. Protein labelling and gel electrophoresis

5.5.6.1. Molecular weight determinations of labeled proteins. WRP were pipetted into wells of tissue culture plates with 10 mg per well for *H. brasiliensis*, 3 mg per well for *P. argentatum* and 1 mg per well for *F. elastica*. The volume of reaction mix was increased to 50 µl with addition of solutions to make final concentrations 50 µM ^{3}H-BzGPP (*p*), 100 mM Tris-HCl, pH 7.5, and 1.75 mM $MgSO_4$. WR from *H. brasiliensis* and *F. elastica* were exposed to UV light for 60 min while WRP rubber particles from *P. argentatum* were exposed for 5 min. Each 50 µl reaction mixture was transferred to a siliconized microfuge tube and 10 µl of WB was used to rinse the well, which was then added to the microfuge tube. To each tube, 17 µl of 4× (WSB) was added, heated at 95 °C for 5 min, and the samples were stored at −20 °C until analysis. The samples were analyzed by 4–20%, 3%, 3.5%, 4%, 4.5% gels, as described in the Gel Electrophoresis section below.

For the analysis of small proteins, WRP were placed in wells of a tissue culture plate with 1 mg per well of *H. brasiliensis* and 3 mg per well of *P. argentatum*. The reaction volume and concentrations of reagents were as described above. UV light exposure was 60 min for *H. brasiliensis* and 30 min for *P. argentatum*. For 15% and 18% gels, two wells (100 µl) from the microtiter plate were combined and 15 µl of 4× Bio-Rad Tris-Glycine sample buffer were added. The samples were heated at 95 °C for 5 min then stored at −20 °C until analysis. For 16.5% gels, 100 µl of Bio-Rad Tris-Tricine sample buffer was added to 50 µl samples.

The molecular weight markers used were Bio-Rad 317 (broad range - 200,000 to 1423 Da). Kaleidoscope standards 324 (broad range - 200,000 to 5500 Da) also were used. The molecular weight markers for large proteins were Sigma cross-linked phosphorylase b molecular weight markers #P8906 (584,400, 487,000, 389,600, 292,000, 194,800, 97,400 Da). The isoelectric focusing (IEF) Standards used were IEF 3-10 (InVitrogen 39212-01), pI 10.7 to 3.5.

Bromophenol Blue was added to both the samples and the molecular weight markers before loading into the sample wells in the stacking gel. For initial analysis on 4–20% Bio-Rad gels, the molecular weight markers and samples were in WSB.

Samples and molecular weight markers were prepared for large molecular weight protein analysis, as described in Bio-Rad Technical bulletin MWS-877x. The sample buffer was 0.028 M sodium phosphate monobasic monohydrate ($NaH_2PO_4{\cdot}H_2O$), 0.072 M sodium phosphate dibasic anhydrous (Na_2HPO_4), 1% SDS (g/100 ml), 0.142 M β-

mercaptoethanol, and 36% (g/100 ml) urea. The buffer was heated at 95 °C for 5 min before use. For samples, 14 mg of urea (36% urea) was added to 40 µl of labeled material in WSB and heated at 95 °C for 5 min.

WSB was used for molecular weight markers and samples for small molecular weight protein analysis using 15% gels so that the Coomassie Blue did not obscure small proteins running at the dye front. For 18% gels, 20 mg of urea was added to each molecular weight marker in WSB and to each sample in Tris-Glycine buffer, then heated at 95 °C for 5 min. For 16.5% gels, 20 mg of urea was added to molecular weight markers and samples in Tris-Tricine sample buffer, and then heated at 95 °C for 5 min.

For interspecific comparisons of small molecular weight proteins, samples were denatured in NuPAGE LDS Sample buffer for 10 min at 95 °C.

IEF samples were prepared in 2× sample buffer (30% glycerol, 2x Cathode buffer) and heated for 20 min at 28 °C.

A Hoefer Scientific Instruments PS 500XT DC Power Supply (Hoefer, San Francisco, CA) and the Bio-Rad Mini 2D gel apparatus (Bio-Rad, Hercules, CA) were used for all gel electrophoresis. The samples were run on a Tris-HCl Ready Gel Precast 10 lane Gel 4–20% linear gradient (Bio-Rad 161-1105), at a constant 100 V for 2 h to ensure that unbound ^{3}H-Bz-GPP (*p*) would be eluted. The gels were loaded as follows: lane 2, Kaleidoscope 324 markers; lane 4, radiolabeled rubber particles; lane 6, molecular weight markers 317; lane 8, labeled rubber particles without tritium. The gel was cut in half. The half containing lanes 1-5 was fixed and placed on Whatman filter paper. The gel half with lanes 6–10 was fixed in methanol, silver-stained and placed on Whatman filter paper.

The small molecular weight proteins were characterized using Tris-HCl Ready Precast 15% Gels (Bio-Rad 161-1103) and 18% (Bio-Rad 161-1216) resolving gels with 4% stacking gels, and Tris-Tricine Ready Gel Precast Gels with a 16.5% resolving gel, and a 4% stacking gel (Bio-Rad 161-1107). The 15% gels were run at a constant 200 V for 30 min; the 18% gels were run at a constant 200 V for 35 min; and the 16.5% gels were run at a constant 200 V for 45 min.

The large molecular weight proteins were characterized using phosphate buffer gels of 3%, 3.5%, 4%, and 4.5% polyacrylamide with a stacking gel using Bio-Rad Mini 2D gel with 1.5 mm plate separators, 15–1.5 mm teeth, as described by Technical bulletin MWS-877x. The running buffer was 0.019 M sodium phosphate monobasic monohydrate, 0.048 M sodium phosphate dibasic anhydrous, 0.07% (g/100 ml) sodium dodecyl sulfate. The stock acrylamide solution was 15% with 14.01 gm acrylamide and 0.37 gm BIS (N,N′-methylene-bis-acrylamide) per 100 ml (filtered and stored in darkness at 4 °C). The gel was run as follows: Lane 1, 5 µl Kaleidoscope 324 standards; Lane 3, Lane 5 and Lane 7, 40 µl of radiolabelled rubber particles; Lane 8, 5 µl of Kaleidoscope 324; Lane 9, 5 µl of Kaleidoscope 324; Lane 11 and Lane 13, 2 µl Sigma phosphorylase b molecular weight standards; and Lane 15, 5 µl Kaleidoscope 324. Gels were run at a constant voltage of 100 V until the dye front reached the bottom of the gel, approximately 60 min. Gels were carefully cut in half between lane 8 and lane 9. The gel half with lanes 1–8 was placed directly onto Whatman paper and dried under vacuum on a Bio-Rad Slab Gel Drier 443 for 60 min at 60 °C until the gel was no longer cool to the touch, indicating that drying was complete. The gel half with lanes 9-15 was fixed and stained with conventional (not fast) Bio-Rad silver stain. The second gel half was then dried as described above.

For interspecific comparisons of small proteins in the WRP, a 12% NuPAGE Novex Bis-Tris gel was run at 200 V for 40 min using the Novex gel system. The buffer was 50 mM MES, 50 mM Tris, 0.1% SDS, 1 mM EDTA, pH 7.2.

Isoelectric focusing was performed using IEF gels, Novex pH 3-10, (InVitrogen EC6655A), standards Novex IEF 3-10 (InVitrogen 39212-01), Novex cathode buffer pH 3-10 10× (InVitrogen LC5310), and Novex IEF anode buffer 50× (InVitrogen LC5300). After the samples were loaded, the gel was run at 100 V for 1 h, 200 V for 38 min, 100 V for 1 h, and 423 V for 35.5 min. The gel was fixed for 1 h in 30% methanol, 10% TCA, and 3.5% sulfosalicylate. The gel was then transferred to 30% methanol, and 12% TCA and left overnight shaking at room temperature. The gel was then silver stained (Bio-Rad silver stain protocol).

5.5.6.2. Analysis of labeled gels using Bioscan 200 imaging scanner. Radiolabeled-polyacrylamide gels were examined using a Bioscan 200 imaging scanner (Bioscan, Inc., 4590 MacArthur Blvd., Washington, D.C. 20007). Data were collected on each lane for up to 8 h. NSCAN and Winscan 2D software were used to evaluate the scans and data files were transferred to Excel (Microsoft) for analysis.

Molecular weight standards were analyzed by adding 0.06 µl of ^{3}H-BzGPP(*p*) to the center of the lane on each silver stained band, at the bottom of the well, and at the dye front or at the bottom of the gel. The scan time for data collection from these standards was 1 min.

5.5.6.3. Molecular weight analysis. Ferguson analysis (Ferguson, 1964) was used to determine the molecular weights of the large proteins, by comparing the negative slope (log R_f vs %acrylamide) vs molecular weight of standards run on 3%, 3.5%, 4% and 4.5% polyacrylamide gels with negative slope of log Rf vs %acrylamide of radiolabeled proteins run on 4% and 4.5% gels.

Small proteins were evaluated by comparison of R_f radiolabeled proteins to R_f standards vs log (molecular weight of standards) on three different gels 15%, 18% and 16.5% polyacrlyamide gels.

5.5.6.4. Gel washing to determine persistence of label. SDS-PAGE gels of labeled proteins were washed for different numbers of times, at room temperature, and scanned.

5.5.6.5. Purification of labeled material. Gel pieces, 1 cm in length, were cut from the scanned gels. Each gel was scanned before and after cutting the 1 cm length pieces; gel pieces confirmed to contain tritium were collected. Using Millipore application 311 for extraction, application 355 for passivation of microcons (YM3,000; YM10,000; YM50,000; YM100,000), and Ultrafree-MC to improve recovery, gel pieces were placed into siliconized 1.5 ml microfuge tubes with 100 µl of extraction buffer (100 mM $NaHCO_3$, 8 M Urea, 3% SDS, 0.5% Triton X-100 [reduced], and 25 mM DTT). Each gel piece was heated for 30 min in a 60 °C water bath. Each gel piece then was homogenized in the microfuge tube with a Kontes Pellet Pestle Motor equipped with a plastic pestle. Each sample then was placed into the 60 °C water bath for another 6.5 h. Samples were stored overnight at 4 °C. Samples were reheated for 4.5 h at 60 °C, transferred into a Millipore Ultrafree-MC microcon, and centrifuged at 13,000 rpm for 5 min. Filter and gel were washed again with 100 µl of extraction buffer, centrifuged, washed with 100 µl of 50% methanol and recentrifuged. The filtered material was placed in a microcon (YM 3000) and centrifuged. The tritiated retentate material from the YM 3000 and/or the tritiated flow-through material were saved and stored at −20 °C. Proteins purified from the gels were rerun on 4–20% gels and scanned for tritium using in the Bioscan 200 Imaging Scanner.

5.5.6.6. Purification and isoelectric focusing of the P. argentatum large protein. Proteins from *P. argentatum* WRP were first solubilized by mixing in 1% SDS on an orbital shaker for 60 min at room temperature and then clarified by centrifugation at 11,950 × *g* for 5 min before collecting the protein-containing supernatant. A 0–80% ammonium sulfate precipitate was collected by centrifugation at 3000 × *g*, after removing the lipid and rubber supra-natent layer. The pellet was resuspended in TE (10 mM Tris pH 8, 1 mM EDTA) and dialyzed overnight at 4 °C against 0.1% Triton X-100 in TE. The dialysate was changed once, and dialysis was continued for 2 h. Dialyzed proteins were loaded onto a 3–8% Tris-Acetate gel, run for 1 h at 150 V, and fixed overnight. The gel was silver stained, and the stained band cut from the gel and electroeluted using Amicon's Centrilutor according to

the manufacturer's directions. The protein was concentrated on a passivated, microcon YM-100,000. The purified proteins were loaded onto IEF gels and run as described above.

Acknowledgements

We wish to thank DuPont for financial support through a USDA-CRADA #58-3K95-8-660, Dr. D.K. Shintani, University of Nevada, Reno, Nevada, for the polyclonal antibodies to *P. argentatum* WRP, and Mr. Z. Li, EnergyEne, Inc., Wooster, Ohio, for the models in Fig. 13, and Dr. J.J. Blakeslee for his critical review of this manuscript. The United States Department of Agriculture, National Institute of Food and Agriculture (Hatch project #230837).

References

Backhaus, R.A., Cornish, K., Chen, S.F., Huang, D.S., Bess, V.H., 1991. Purification and characterization of an abundant rubber particle protein from guayule. Phytochemistry 30, 2493–7249.

Benedict, C.R., Madhavan, S., Greenblatt, G.A., Venkatachalam, K.V., Foster, M.A., 1990. The enzymatic synthesis of rubber polymer in *Parthenium argentatum* Gray. Plant Physiol. 92, 816–821.

Berthelot, K., Lecomte, S., Estevez, Y., Zhendre, V., Henry, S., Thevenot, J., Dufourc, E.J., Alves, I.D., Peruch, F., 2014. Rubber particle proteins, HbREF and HbSRPP, show different interactions with model membranes. Biochim. Biophys. Acta 1838, 287–299.

Collins-Silva, J., Nural, A.S., Skaggs, A., Scott, D.J., Hathwai, U., Woolsey, R., Schegg, K., McMahan, C.M., Whalen, M., Cornish, K., Shintani, D.K., 2012. Altered levels of the *Taraxacum kok-saghyz* (Russian dandelion) small rubber particle protein, TkSRPP3, result in qualitative and quantitative changes in rubber metabolism. Phytochemistry 79, 46–56.

Cornish, K., 1993. The separate roles of plant *cis* and *trans* prenyl transferases in *cis*-1,4-polyisoprene biosynthesis. Eur. J. Biochem. 218, 267–271.

Cornish, K., 2001a. Biochemistry of natural rubber, a vital raw material, emphasizing biosynthetic rate, molecular weight and compartmentalization, in evolutionarily divergent plant species. Nat. Prod. Rep. 18, 182–227.

Cornish, K., 2001b. Similarities and differences in rubber biochemistry among plant species. Phytochemistry 57, 1123–1134.

Cornish, K., Backhaus, R.A., 1990. Rubber transferase-activity in rubber particles of guayule. Phytochemistry 29, 3809–3813.

Cornish, K., Bartlett, D.L., 1997. Stabilisation of particle integrity and particle bound *cis*-prenyl transferase activity in stored, purified rubber particles. Phytochem. Anal. 8, 130–134.

Cornish, K., Siler, D.J., 1996. Characterization of *cis*-prenyl transferase activity localised in a buoyant fraction of rubber particles from *Ficus elastica* latex. Plant Physiol. Biochem. 34, 377–384.

Cornish, K., Siler, D.J., Grosjean, O.K., Goodman, N., 1993. Fundamental similarities in rubber particle architecture and function in three evolutionarily divergent plant species. J. Nat. Rubber Res. 8, 275–285.

Cornish, K., Siler, D.J., Grosjean, O.K., 1994. Immuno inhibition of rubber particle-bound *cis*-prenyl transferases in *Ficus elastica* and *Parthenium argentatum*. Phytochemistry 35, 1425–1428.

Cornish, K., Wood, D.F., Windle, J.J., 1999. Rubber particles from four different species, examined by transmission electron microscopy and electron-paramagnetic-resonance spin labeling, are found to consist of a homogeneous rubber core enclosed by a contiguous, monolayer biomembrane. Planta 210, 85–96.

Dennis, M.S., Light, D.R., 1989. Rubber elongation factor from Hevea brasiliensis. Identification, characterization and role in rubber biosynthesis. J. Biol. Chem. 264, 18608–18617.

Dorman, G., Prestwich, G.D., 1994. Benzophenone photophores in biochemistry. Biochemistry 33, 5661–5673.

Dorman, G., Prestwich, G.D., 2000. Using photolabile ligands in drug discovery and development. Trends Biotechnol. 18, 64–77.

Dorman, G., Nakamura, H., Pulsipher, A., Prestwich, G.D., 2016. The life of pi star: exploring the exciting and forbidden worlds of the benzophenone photophore. Chem. Rev. 116, 15284–15398.

Espy, S.C., Keasling, J.D., Castillon, J., Cornish, K., 2006. Initiator-independent and initiator-dependent rubber biosynthesis in *Ficus elastica*. Arch. Biochem. Biophys. 448, 13–22.

Ferguson, K.A., 1964. Starch-gel electrophoresis- application to the classification of pituitary proteins and polypeptides. Metabolism 13, 1985–2002.

Fujihashi, M., Zhang, Y.W., Higuchi, Y., Li, X.Y., Koyama, T., Miki, K., 2001. Crystal structure of *cis*-prenyl chain elongating enzyme, undecaprenyl diphosphate synthase. Proc. Natl. Acad. Sci. Unit. States Am. 98, 4337–4342.

Gaon, I., Turek, T.C., Distefano, M.D., 1996a. Farnesyl and geranylgeranyl pyrophosphate analogs incorporating benzoylbenzyl ethers: synthesis and inhibition of yeast protein farnesyltransferase. Biochemistry 37, 8833–8836.

Gaon, I., Turek, T.C., Weller, V.A., Edelstein, R., Singh, S.K., Distefano, M.D., 1996b. Photoactive analogs of farnesyl pyrophosphate containing benzoylbenzoate esters: synthesis and application to photoaffinity labeling of yeast protein farnesyltransferase. J. Org. Chem. 61, 7738–7745.

Ko, T.P., Chen, Y.K., Robinson, H., Tsai, P.C., Gao, Y.G., Chen, A.P., Wang, A.H., Liang, P.H., 2001. Mechanism of product chain length determination and the role of a flexible loop in *Escherichia coli* undecaprenyl-pyrophosphate synthase catalysis. J. Biol. Chem. 276, 47474–47482.

Laibach, N., Hillebrand, A., Twyman, R.M., Prüfer, D., Schulze, T., Gronover, C.N., 2015. Identification of a *Taraxacum brevicorniculatum* rubber elongation factor protein that is localized on rubber particles and promotes rubber biosynthesis. Plant J. 82, 609–620.

Light, D.R., Dennis, M.S., 1989. Purification of a prenyltransferase that elongates *cis*-polyisoprene rubber from the latex of *Hevea brasiliensis*. J. Biol. Chem. 264, 18589–18597.

Light, D.R., Lazarus, R.A., Dennis, M.S., 1989. Rubber elongation by farnesyl pyrophosphate synthases involves a novel switch in enzyme stereospecificity. J. Biol. Chem. 264, 18598–18607.

Madhavan, S., Greenblatt, G.A., Foster, M.A., Benedict, C.R., 1989. Stimulation of isopentenyl pyrophosphate incorporation into polyisoprene in extracts from guayule plants (*Parthenium argentatum* Gray) by low temperature and 2-(3,4-dichloro-phenoxy)triethylamine. Plant Physiol. 89, 506–511.

Marecak, D.M., Horiuchi, Y., Arai, H., Shimonaga, M., Maki, Y., Koyama, T., Ogura, K., Prestwich, G.D., 1997. Benzoylphenoxy analogs of isoprenoid diphosphates as photoactivatable substrates for bacterial prenyltransferases. Bioorg. Med. Chem. Lett 7, 1973–1978.

Mau, C.J.D., Scott, D.J., Cornish, K., 2000. Multiwell filtration system results in rapid, high-throughput rubber transferase microassay. Phytochem. Anal. 11, 356–361.

Mau, C.J.D., Garneau, S., Scholte, A.A., Van Fleet, J.E., Vederas, J.C., Cornish, K., 2003. Protein farnesyltransferase inhibitors interfere with farnesyl diphosphate binding by rubber transferase. Eur. J. Biochem. 270, 3939–3945.

Pan, Z.Q., Durst, F., Werck-Reichhart, D., Gardner, H.W., Camara, B., Cornish, K., Backhaus, R.A., 1995. The major protein of guayule rubber particles is a cytochrome-P450-characterization based on cDNA cloning and spectroscopic analysis of the solubilized enzyme and its reaction-products. J. Biol. Chem. 270, 8487–8494.

Post, J., Van Deenen, N., Fricke, J., Kowalski, N., Wurbs, D., Schaller, H., Eisenreich, W., Huber, C., Twyman, R.C., Prüfer, D., Gronover, C.S., 2012. Laticifer specific *cis*-prenyltransferase silencing affects the rubber, triterpene and inulin content of *Taraxacum brevicorniculatum*. Plant Physiol. 154, 1406–1417.

Qu, Y., Chakrabarty, R., Tran, H.T., Kwon, E.-J.G., Kwon, M., Nguyen, T.-D., Ro, D.-K., 2015. A lettuce (*Lactuca sativa*) homolog of human Nogo-B receptor interacts with *cis*-prenyltransferase and is necessary for natural rubber biosynthesis. J. Biol. Chem. 290, 1898–1914.

Rodbard, D., Chrambach, A., 1970. Unified theory of gel electrophoresis and gel filtration. Proc. Natl. Acad. Sci. Unit. States Am. 65, 970–977.

Rodbard, D., Chrambach, A., 1971. Estimation of molecular radius, free mobility, and valence using polyacrylamide gel electrophoresis. Anal. Biochem. 40, 95–134.

Schmidt, T., Hillebrand, A., Wurbs, D., Wahler, D., Lenders, M., Gronover, C.S., Prüfer, D., 2010a. Molecular cloning and characterization of rubber biosynthetic genes from *Taraxacum koksaghyz*. Plant Mol. Biol. Rep. 28, 277–284.

Schmidt, T., Lenders, M., Hillebrand, A., van Deenen, N., Munt, O., Reichelt, R., Eisenreich, W., Fischer, R., Prüfer, D., 2010b. Characterization of rubber particles and rubber chain elongation in *Taraxacum koksaghyz*. BMC Biochem. 11, 1–11.

Scott, D.J., Da Costa, B.M.T., Espy, S.C., Keasling, J.D., Cornish, K., 2003. Activation and inhibition of rubber transferases by metal cofactors and pyrophosphate substrates. Phytochemistry 64, 123–134.

Shanklin, J., Somerville, C., 1991. Stearoyl-acyl-Carrier-protein desaturase from higher plants is structurally unrelated to the animal and fungal homologs. Proc. Natl. Acad. Sci. Unit. States Am. 88, 2510–2514.

Siler, D.J., Cornish, K., 1993. A protein from *Ficus elastica* rubber particles is related to proteins from *Hevea brasiliensis* and *Parthenium argentatum*. Phytochemistry 32, 1097–1102.

Siler, D.J., Cornish, K., 1994. Identification of *Parthenium argentatum* rubber particle proteins immunoprecipitated by an antibody that specifically inhibits rubber transferase activity. Phytochemistry 36, 623–627.

Siler, D.J., Goodrich-Tanrikulu, M., Cornish, K., Stafford, A.E., Mckeon, T.A., 1997. Composition of rubber particles of *Hevea brasiliensis, Parthenium argentatum, Ficus elastica*, and *Euphorbia lactiflua* indicates unconventional surface structure. Plant Physiol. Biochem. 35, 881–889.

Tarshis, L.C., Yan, M., Poulter, C.D., Sacchettini, J.C., 1994. Crystal structure of recombinant farnesyl diphosphate synthase at 2.6Å resolution. Biochemistry 33, 10871–10877.

Tong, Z., Wang, D., Sun, Y., Yang, Q., Meng, X., Wang, L., Feng, W., Li, L., Wurtele, E.S., Wang, X., 2017. Comparative proteomics of rubber latex revealed multiple protein species of REF/SRPP family respond diversely to ethylene stimulation among different rubber tree clones. Int. J. Mol. Sci. 18, 958–972.

Turek-Etienne, T.C., Strickland, C.L., Distefano, M.D., 2003. Biochemical and structural studies with prenyl diphosphate analogues provide insights into isoprenoid recognition by protein farnesyl transferase. Biochemistry 42, 3716–3724.

Wadeesirisak, K., Castano, S., Berthelot, K., Vaysse, L., Bonfils, F., Peruch, F., Rattanaporn, K., Liengprayoon, S., Lecomte, S., Bottier, C., 2017. Rubber particle proteins REF1 and SRPP1 interact differently with native lipids extracted from *Hevea brasiliensis* latex. Biochim. Biophys. Acta 1859, 201–210.

Wititsuwannakul, D., Rattanapittayaporn, A., Koyama, T., Wititsuwannakul, R., 2004. Involvement of Hevea latex organelle membrane proteins in the rubber biosynthesis activity and regulatory function. Macromol. Biosci. 4, 314–323.

Wood, D.F., Cornish, K., 2000. Microstructure of purified rubber particles. Int. J. Plant Sci. 161, 435–445.

Yamashita, S., Yamaguchi, H., Waki, T., Aoki, Y., Mizuno, M., Yanbe, F., Ishii, T., Funaki, A., Tozawa, Y., Miyagi-Inoue, Y., Fushihara, K., Nakayama, T., Takahashi, S., 2016.

Identification and reconstitution of the rubber biosynthetic machinery on rubber particles from *Hevea brasiliensis*. Biochem. Chem. Biol. Plant Biol. eLife 2016, 5 e19022.
Ying, W., Sepp-Lorenzino, L., Cai, K., Aloise, P., Coleman, P.S., 1994. J. Biol. Chem. 269, 470–477.
Zhang, Y.W., Koyama, T., Marecak, D.M., Prestwich, G.D., Maki, Y.J., Ogura, K., 1998. Two subunits of heptaprenyl diphosphate synthase of *Bacillus subtilis* form a catalytically active complex. Biochemistry 37, 13411–13420.